Department of Chemistry, University of Jyväskylä

ULTRAFAST LIGHT INDUCED DISSOCIATION OF $RU(DCBPY)(CO)_2I_2$ IN SOLUTION

Viivi Lehtovuori

Academic Dissertation
for the Degree of
Doctor of Philosophy

Jyväskylä, Finland 2004

Research Report No. 106

SUPERVISOR

Prof. Jouko Korppi-Tommola

Department of Chemistry, University of Jyväskylä, Finland

OPPONENT

Prof. Villy Sundström

Department of Chemical Physics, Lund University, Sweden

REVIEWERS

Dr. Jennifer Herek

FOM Institute for Atomic and Molecular Physics, AMOLF, The Netherlands

Dr. Maxim S. Pshenichnikov

Department of Chemical Physics, University of Groningen, The Netherlands

DEPARTMENT OF CHEMISTRY, UNIVERSITY OF JYVÄSKYLÄ
RESEARCH REPORT No. 106

ULTRAFAST LIGHT INDUCED DISSOCIATION OF RU(DCBPY)$(CO)_2I_2$ IN SOLUTION

BY

VIIVI LEHTOVUORI

Academic Dissertation
for the degree of
Doctor of Philosophy

To be presented, by permission of the Faculty of Mathematics and Science of the University of Jyväskylä, for public examination in Auditorium FYS 1, on 16th April, 2004, at 12 noon

Jyväskylä, Finland
ISBN 951-39-1764-9
ISSN 0357-346X

URN:ISBN:978-951-39-9976-6
ISBN 978-951-39-9976-6 (PDF)
ISSN 0357-346X

Jyväskylän yliopisto, 2024

It's dangerous business, Frodo, going out of your door.
You step into the Road, and if you don't keep your feet
there is no knowing where you might be swept off to.
-Bilbo Baggins

Preface

This work has been carried out between the years 1998 and 2003 in the Department of Chemistry, University of Jyväskylä. Part of the experiments were carried out in Max Born Institute für Nichtlineare Optik und Kurzzeit Spektroskopie in Berlin and in National Laboratory for Ultrafast and Ultraintense Optical Science in Politecnico di Milano.

First of all I would like to thank my supervisor prof. Jouko Korppi–Tommola for giving me opportunity to carry out this work – your enthusiasm and faith in my skills made this all possible. I am also grateful to prof. Henrik Kunttu. I greatly appreciate your support especially during the last steps of this work.

Maybe the most important results of this thesis were obtained during my visits in Berlin and in Milan. In Berlin I would like to thank Dr. Erik Nibbering and Dr. Matteo Rini for introducing me the basics of transient IR experiments and helping me with the data. I would also like to mention the excellent local guide that I had during the Berlin weeks, thank's Toni. I am deeply indebted to prof. Giulio Cerullo, Cristian Manzoni and Dario Polli in Milan. Your persistent help in lab and kindness made the visits in Politecnico a great joy. Dr. Matti Haukka in University of Joensuu deserves special thanks for providing me "my dear rutheniums" during these years, sometimes even with a very short notice. I want also thank Matti and Juha for carrying out calculations that greatly helped us to understand the experimental data.

The femtogroup, "my boys", Jani, Pasi, Janne S. and Jukka, I want to thank you for the nice times and for all your help in and outside of the dark lab and for the pleasant company in our various trips all around the world. It has been a privilege to work with you. Our small but intensive physical chemistry department has been a very special working environment. Saara, Heikki, Janne I., Mikko, Jari, Jussi and all the others: thank you for creating this inspiring atmosphere –also outside of the coffee room.

My parents, my brother, my friends, Martat and all those numerous nice colleagues I have met during the course of this work. I wouldn't be here without you; you made this worth it.

Financial support from Academy of Finland and European Commission is acknowledged.

Last but not least, Pekka, thank you for being there and delighting my days.

Jyväskylä, March 2004
Viivi Lehtovuori

Abstract

The research presented in this thesis focuses on the characterization of a detailed mechanism of the light induced ligand exchange reaction of (*trans*-I)Ru(dcbpy)$(CO)_2I_2$, (dcbpy= 4,4'-dicarboxy-2,2'-bipyridine). Illumination of Ru(dcbpy)$I_2(CO)_2$ with (near)ultraviolet light (UV) induces dissociation of one of the CO groups of the complex. In solution the opened coordination site of the metal is occupied by a solvent molecule. The starting point of this work was structural and spectral characterization of both the reactant and the product complexes and their electronic states. The main experimental technique utilized was transient absorption spectroscopy. The parent molecules were excited with a UV pulse and the dynamics of the ongoing reaction was recorded in the visible and in the infrared spectral regions. Based on the results of these measurements and quantum chemical calculations the following model for the ligand exchange reaction is suggested. The UV photon at 320 nm prepares the molecule in a dcbpy ligand centered $\pi^* \leftarrow \pi$ state. From this state internal conversion to a lower lying bound state and a repulsive state takes place with a time constant of few tens of fs. Dissociation was considered to have taken place when the CO group has escaped from the first solvation shell. Dissociation competes with geminate recombination and the observed rate constant of 1/62 fs^{-1} is a sum of these two processes. After dissociation ligands of the five-coordinated intermediate rearrange. An iodine ligand occupying initially an axial site moves towards the vacant equatorial site with a time constant of 500 fs. Simultaneously to this a solvent molecule attaches to the opened axial site to form the final product (*cis*-I)Ru(dcbpy)(CO)(EtOH)I_2. Only an excitation wavelength dependent fraction of the excited molecules form the final product. The rest recombine with the five-coordinated intermediate due to cage effect provided by the solvent and reform the parent molecules in less than 170 fs. Also parallel internal conversion to non-reactive states decrease the quantum yield. In the picosecond timescale excess energy of the system undergoes intramolecular vibrational energy redistribution among the several vibrational modes of the newly born product and the recombined reactant and finally is dissipated as heat into the solvent environment. One important observation in this work was the survival of the excited state coherence over the duration of the dissociation reaction.

Original publications

This thesis is a review based on the following original research papers.

- **I Photochemical reactivity of halogen-containing ruthenium-dcbpy (dcbpy=4,4'-dicarboxylic acid-2,2'-bipyridine)compounds, *trans*(Br)-[Ru(dcbpy)$(CO)_2Br_2$ and *trans*(I)-[Ru(dcbpy)$(CO)_2I_2$**
  Saija Luukkanen, Matti Haukka, Esa Eskelinen, Tapani A. Pakkanen, Viivi Lehtovuori, Jani Kallioinen, Pasi Myllyperkiö, and Jouko Korppi-Tommola
  Phys. Chem. Chem. Phys. **2001**, *3*, 1992.
  https://doi.org/10.1039/B100659M

- **II Effects of ligand substitution on the excited state dynamics of the Ru(dcbpy)$(CO)_2I_2$ complex**
  Viivi Lehtovuori, Jani Kallioinen, Pasi Mylllyperkiö, Matti Haukka, and Jouko Korppi-Tommola
  Chem. Phys. **2003**, *295*, 81.
  https://doi.org/10.1016/j.chemphys.2003.08.008

- **III Transient Midinfrared study of light induced dissociation reaction of Ru(dcbpy)$(CO)_2I_2$ in solution**
  Viivi Lehtovuori, Jukka Aumanen, Pasi Myllyperkiö, Matteo Rini, Erik T.J. Nibbering, and Jouko Korppi-Tommola
  J. Phys. Chem. A, **2004**, *108*, 1644.
  https://doi.org/10.1021/jp036492u

- **IV A study of mechanisms of light induced dissociation of Ru(dcbpy)$(CO)_2I_2$ in solution with 20 fs time resolution**
  Viivi Lehtovuori, Pasi Myllyperkiö, Juha Linnanto, Cristian Manzoni, Dario Polli,Giulio Cerullo, Matti Haukka and Jouko Korppi-Tommola
  J. Am. Chem. Soc., submitted.
  https://doi.org/10.1021/jp044735s

Abbreviations

BBO = β-Barium-borate (non-linear crystal)
bpy = 2,2'-bipyridine
ΔA= Change in Absorption
dcbpy = 4,4'-dicarboxy-2,2'-bipyridine
Cp =Cyclopentadienyl
fs = Femtosecond (1×10^{-15}s)
IC = Internal Conversion
IR = Infrared
IVR = Intramolecular Vibrational energy Redistribution
LC = Ligand Centered
LF = Ligand Field = MC
MC = Metal Centered
MLCT = Metal-to-Ligand Charge Transfer
NOPA = Non-Collinear Optical Parametric Amplification
ps = Picosecond (1×10^{-12}s)
SHG = Second Harmonic Generation
UV = Ultraviolet (200-400 nm)
XLCT =Halogen-to-Ligand Charge Transfer

Contents

Chapter 1

Introduction

In this chapter a short introduction to transition metal complexes and their reactions is given. The first section will shortly describe a background and a motivation to why it is interesting to study transition metal complexes, and especially their photoinduced reactions. The purpose of this chapter is not to give a broad literature overview but more to introduce the field and its phenomena.

1.1 Motivation

Due their unique redox properties, excited state lifetime and reactivity transition metal pyridyls have attracted great interest since the first observation of room temperature luminescence of $Ru(bpy)_3^{2+}$ in 1959 by Paris and Brandt.[1–4] Densely packed electronic states with generally strong mixing of states is a typical feature of these complexes.[5] In addition, excitation of transition metal complexes generates often electron deficiency on the metal states of the complex making the metal formally oxidized compared to the ground state. At the same time increased electron density on the ligand orbitals results in enhanced reducing ability. Therefore, the excited state is both better oxidant and reductant than the ground state. Both the excited and the ground state properties determine the photochemical and photophysical activities. One promising field of photoactivation utilizing redox properties of transition metal complexes is solar energy conversion. Sensitization of nanocrystalline wide band-gap semiconductor films with dye molecules has been proved as cost-effective solution for dye-sensitized solar cells. For the present ruthenium bipyridine complexes on TiO_2 surface has shown the best

solar energy to electricity conversion efficiency of ~10 %.[6,7]

Another motivation to study of transition metal complexes, especially transition metal carbonyls, is their use as catalysts in several synthetic reactions.[8] Typically the role of metal carbonyls in these reactions is to open a vacant coordination site for other reactants. For example, in catalytic hydrogenation of alkenes metal carbonyl catalyst both activates the relatively strong H-H bond and serves as a template where both reacting species can unite.[9] Other type of reactions that can be photocatalyzed by metal carbonyls are for example hydrosilation and isomerization of alkenes, carbonylation of alkanes or aromatic hydrocarbons.[8,10–14] One important reaction that is catalyzed by transition metal carbonyls is water gas shift reaction, that is the reaction of water with carbon monoxide to form hydrogen and carbon dioxide. The interest in this reaction lies in its potential use as a hydrogen source in conjunction with fuel cell power generation.

An advantage of photochemical activation of molecules compared to thermal activation is that milder reaction conditions with respect to temperature and pressure are required, and hence the undesirable side reactions are minimized. Furthermore, the number of thermodynamically favorable products of photochemical reactions is greater than that can be obtained from thermal reactions. This is mainly because the light pulse generates selectively a high energy intermediate, which is capable of reacting further leading to formation of the desired product(s). An ideal case would be that by selecting the wavelength and pulse shape it would be possible to tune the photochemical reactivity and switch between different reaction pathways such as dissociation/substitution/reorganization. Nowadays this is possible by utilizing a technique called coherent control.[15] For example, $CpFe(CO)_2Cl$ (Cp=cyclopentadienyl) undergoes a photoinduced dissociation reaction. By varying the phase of different wavelengths of the excitation pulse different fragmentation channels may be selected leading to different products, such as $CpFe(CO)Cl^+$ (cleavage of one Fe-CO bond) or $FeCl^+$ (cleavage of two Fe-CO bonds and a Cp group).[16]

Femtosecond transient absorption spectroscopy provides a powerful method to investigate the dynamics and intermediate states of such reactions. Variation of the excitation and the probe wavelengths and combining the results obtained from these experiments with the results from quantum chemical calculations, wavepacket simulations and steady state spectroscopy gives an insight into the excited states involved, transition rates between the states and finally the mechanism of the overall reaction. This information is useful for example in the design of new and more efficient catalysts. Also from the

point of view of basic science revealing what are the active vibrational modes in the reaction and the mechanism how the bond breakage occurs as well as characterization of different intermediate states of a chemical reaction is very fascinating.

1.2 Electronic States of Transition Metal Complexes

Ligand field theory provides the simplest way of discussing bonding and the lowest energy transitions in transition metal complexes. Many of these complexes posses octahedral binding symmetry, where the d orbitals of the metal are split into occupied t_{2g} and unoccupied e_g orbitals (Figure 1.1). Radius and charge of the central metal as well as chemical nature of the ligands determine the energy separation of these orbitals and the degree of mixing with the ligand orbitals.[5,17] The lowest energy transitions of such complexes may be classified as transitions that mainly occur between the orbitals of the ligand(s) (LC) or those that are centered to metal orbitals (MC or ligand field LF). Metal-to-ligand charge transfer transitions (MLCT) involve promotion of the electrons from the metal to the ligand orbitals (see Figure 1.1). All the excited states may have singlet or triplet multiplicity. Going down from first row transition metals to second and third row metals ligand field splitting (Δ), that is the energy difference between the t_{2g} and e_g orbitals, increases.[2,3] Another important feature is the increase of spin-orbit coupling as the number of electrons in the metal increases. The coupling results in singlet-triplet mixing of the MC and MLCT excited states.[2,3] Furthermore, as spin-orbit coupling increases spin selection rules become less restrictive and spin forbidden singlet triplet transitions become weakly allowed.[5] The relative energies of the LC, MC and MLCT excited states depend on the ligand field strength, the redox properties of the metal and the ligands as well as on the intrinsic properties of the ligands.[2] For example by varying the halide ligand of $Ru(X)(R)(CO)_2(bpy)$ (X=halide, R=alkyl) from chlorine to iodine changes the character of the lowest energy transition from Ru $\rightarrow$ bpy (MLCT) to X $\rightarrow$ bpy (XLCT).[18] On the other hand, electron rich ligands, such as halogens, introduce mixing of the orbitals in such a way that the highest occupied orbitals have contribution both form the the metal d orbital and the π orbitals of the ligands (e.g. -NCS or halogens).[19,20]

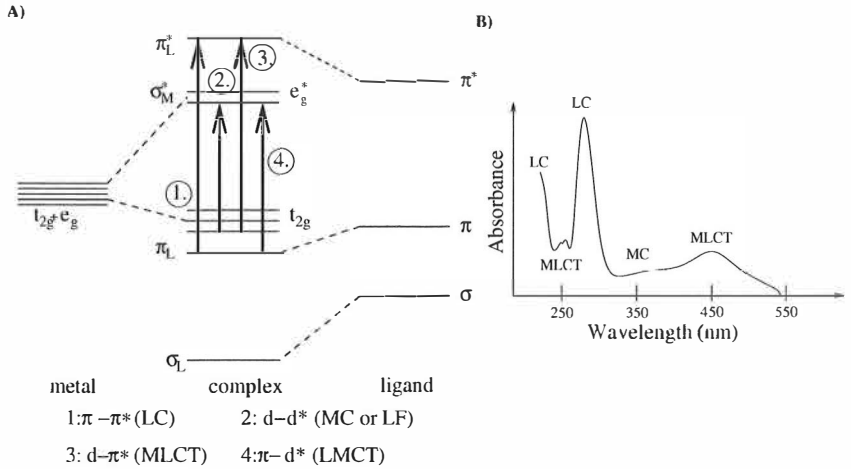

Figure 1.1: A. Relative positions of the metal and the ligand orbital energies and possible electronic transitions in an octahedral ligand field of a transition metal complex B. UV-Vis spectrum of $[Ru(bpy)_3]^+$ in aqueous solution together with assignment of the transitions.[5]

Decay of the excited states may proceed via radiative (luminescent) or non-radiative routes. Moreover, photochemical processes such as energy or electron transfer or substitution reactions of the coordinated ligands may be in charge of the excited state quenching. Energy transfer can, in principle, occur from any type of state but electron transfer usually proceeds via charge transfer states (CT).[5] The excited state reactivity can often be attributed to MLCT state and to the properties of the oxidized metal or the reduced ligand. The increased positive charge at the metal atom facilitate reactions with nucleophiles and may lead to associative ligand substitution reactions (M-L ← M-L'). Decreased electron density around the metal center may also lead to weakening of metal-metal σ bond in bimetallic complexes and finally to dissociation of the bond. MLCT excitation promotes an electron to π^* orbital of the ligand which is strongly antibonding with regard to metal-ligand π interaction. In the organometallic complexes with a metal in low oxidation state this may lead to ligand dissociation. It is also possible that the reduced ligand may undergo photoisomerization or transformations due to electrophilic attack at the reduced ligand.[21,22]

1.3 Photoinduced Dissociation Reactions

Processes of bond formation and bond breaking are at the heart of chemistry. In certain compounds illumination with light induces bond breakage, which may be followed by other reactions such as bond formation or isomerization. By using short light pulses for excitation it is possible to dissociate a bond of a molecule and observe the formation of reaction products in real time as Zewail and coworkers did in their pioneering work of photofragmentation of ICN on the femtosecond time scale.[23]

Transition metal complexes having CO ligands readily undergo dissociation reaction under illumination with ultraviolet (UV) light and that is why very often simple metal carbonyls $M(CO)_n$ have been studied as model compounds in photodissociation studies.[24–28] In the gas phase, elimination of the first CO group is followed by thermal dissociation of further CO ligands,[24,29–31] while in solution the excess thermal energy is dissipated by vibrational cooling and the vacant site in the coordination sphere of the metal center is reoccupied by a solvent molecule.[32–34] The questions then arise what states are involved in the fragmentation process and in the case of $M(CO)_n$ complexes in the gas phase how synchronously the metal-CO bonds are cleaved. In general, photodissociation may involve population of repulsive excited state potential surface or dissociation may take place via the highly excited vibronic states of the ground state potential surface. According to earlier studies of transition metal carbonyls, dissociation of the first carbonyl group is an extremely fast process (<100 fs).[26,27,35–39] The fs cleavage dynamics exclude the possibility of ground state dissociation because time scale of dissociation is shorter than that of most vibrational motions needed to complete internal conversion (IC) and intramolecular vibrational redistribution (IVR).[40]

The highest occupied molecular orbital of a CO ligand is a non-bonding σ orbital. In transition metal carbonyls the metal-CO bond is formed when CO ligand donates the non-bonding σ electrons to the metal and the excess electron density around the metal atom is donated back to the empty π orbitals of the ligand. According to ligand field theory the lowest energy transition in $M(CO)_n$ complexes occurs from occupied metal t_{2g} orbitals to an antibonding metal-ligand e_g orbitals leading to dissociation of a CO ligand.[17] The ligand field excited states may be thought as $d\sigma^*$ states since e_g orbitals are antibonding between the metal d orbitals and σ orbital of the ligand. Hence $d\sigma^*$ state is repulsive along the entire dissociation coordinate. On the other hand, excitation can be considered as electron transfer to an orbital in the same region of space as the metal-ligand σ bond. Then disso-

ciation occurs due to electrostatic repulsion. However, the recent quantum chemical calculation have shown that often π^* orbitals of the ligands (CO or for example bpy) lie lower in energy than the virtual metal orbitals.[25,41,42] Especially in the complexes with α-diimine ligands (such as bpy) the lowest lying excited state is almost completely localized to π^* orbital of a α-diimine ligand. The LF states have much higher energy at the equilibrium geometry but due to their strongly dissociative nature the energy lowers very rapidly upon bond lengthening. The CO dissociative nature of MLCT state may then rise from the avoided crossing of MLCT state with strongly repulsive LF state.[24,25,42] It has been also suggested that in the mixed ligand transition metal complexes states involving charge transfer form metal orbitals to orbitals of axial carbonyls with net decrease of electron density on the metal atom are in charge of the dissociation.[43]

In the complexes with carbonyl groups both in the axial and in the equatorial positions it seems that the ligand field determines which is the weakest bond and the first one to dissociate.[41,42,44–47] It has been observed that dissociation of an equatorial CO results in strong rearrangement of the remaining ligands around the metal center, while no such reorganization is seen after axial dissociation.[24,25,41,48] Quantum chemical calculations and transient absorption measurements of $Cr(CO)_6$ has shown that ligand-metal-ligand bending mode becomes dominant vibrational mode when equatorial CO ligand has left.[24,25] This indicates that the activated vibration leads to bending of the axial ligand towards the vacant equatorial site. In $M(CO)_6$ complexes the conformation change may be explained in terms of pseudo-rotation i.e. interconversion of trigonal pyramid structure trough an intermediate tetragonal pyramid structure typical for all five-coordinated transition metal complexes.[49] Figure 1.2 shows schematic potential energy surfaces which leads to dissociation of $Cr(CO)_6$ in an excited state. The five-coordinated intermediate $Cr(CO)_5$re has three equivalent minimum geometry structures with square pyramidal symmetry, which form a "moat" in the potential energy surface around the conical intersection point. Coupling between the components of degenerate electronic state define whether the molecule can freely pseudo-rotate in the "moat" or is there barriers between the various equivalent local minima.[25]

In the gas phase decarbonylation dynamics is dominated by loss of multiple CO groups. The excess energy brought to the system by the UV excitation is sufficient to dissociate several ligands in contrast to solution phase where the excess energy is dissipated into the environment. As discussed above

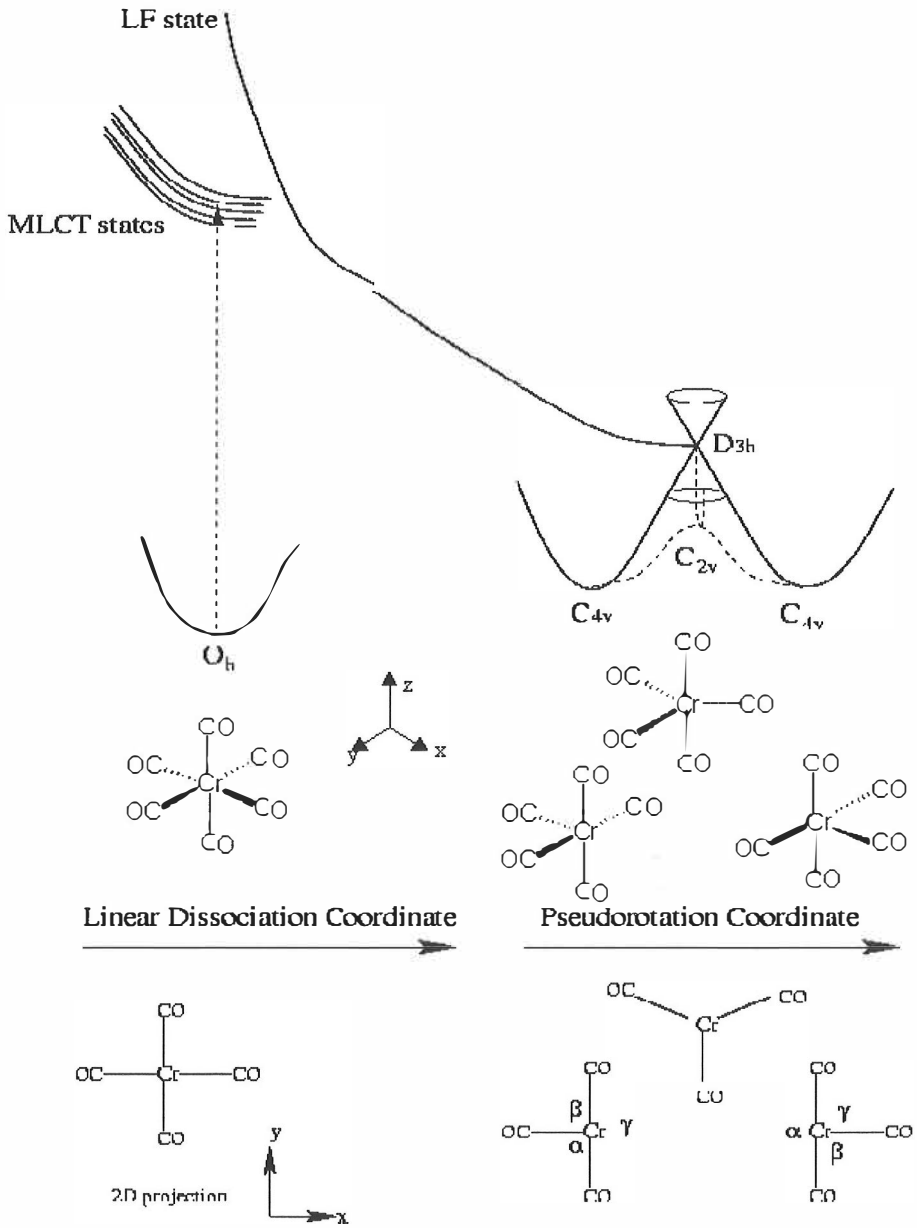

Figure 1.2: Schematic potential surface leading to dissociation of $Cr(CO)_6$ in an excited state. Subsequent decay to the ground state of $Cr(CO)_5$ occurs via conical intersection with D_{3h} symmetry at trigonal bipyramid geometry. Then the molecule can pseudo-rotate in the moat of the conical intersection. The pseudo-rotation coordinate is an antisymmetric bend of three in-plane ligands.[25]

the loss of the first carbonyl is a complicated process involving several excited states and is completed in 100 fs. In the binuclear metal complexes the metal-CO bond dissociation is faster than metal-metal bond dissociation even though the metal-metal bond energy is roughly the same as metal-CO bond energy. The faster dissociation rate for metal-CO bond may be explained with the greater recoil velocity of the smaller dissociating species, which is in accordance with simple kinematics.[29] Depending on the ligands, excitation wavelength or intensity, the dissociation of further COs can proceed either sequentially or in concerted manner.[28,50] The main difference between these two dissociating channels is that in the sequential process the observation of intermediates is possible. If the excitation energy intensity is high enough $Cr(CO)_6$ absorbs two, three or more photons coherently, which leads to dissociation of several CO groups simultaneously in the timescale of a single vibration.[51] If the excitation energy intensity is decreased a stepwise dissociation mechanism becomes more important. For $CpFe(CO)_2X$ (Cp=cyclopentadienyl, X=Cl, Br or I) complex it was observed that the overall fragmentation of the molecule is slowest for the X=Cl species and fastest for X=I species. Furthermore, the complex with Cl ligand shows sequential dissociation steps while in the complexes with heavier halogens the dissociation occurs in concerted and more complicated manner involving also dissociation of halogen or Cp ligands. The reason for different dissociation processes may lie on more effective electron backtransfer mechanism in the lighter halogen ligands which may stabilize intermediate species.[37]

1.4 Ligand Exchange Reactions in Transition Metal Complexes

In light induced reactions of transition metal carbonyl complexes in solution only one CO group is dissociated. The primary photoproduct is a five-coordinated species, which is readily solvated. The solvent molecule or another nucleophile present in the solution coordinates to the vacant site. In the matrix isolation studies the formation of the solvent complex is observed even in inert medium such as Ar or N_2.[52] In the presence of Lewis bases the solvent complex can react further and the solvent ligand may be replaced by a Lewis base.[53,54] It has been suggested that solvent coordination occurs before equilibrium is established, and the structure of the solvated complex is initially determined by the statistical nature of the solvation process.[55,56] Then the complex rearranges to form the most stable nuclear configuration on a slower time scale. However, Harris and coworkers observed that in

ethanol $Cr(CO)_5$ is preferably solvated via the hydroxyl end of the solvent and therefore the solvation process does not follow statistical behavior.[56] The initial solvent coordination takes place within a few ps or less.[34,35,39,55,57–59] Possible rearrangement of the solvent ligand to form the most stable complex takes then from tens to hundreds of ps.[55]

Typically in solution the quantum yield of the reaction is less than unity.[48,58] The reason for the non-unity quantum yield may be that IC to a nonreactive state competes with the CO dissociation or that a fraction of the dissociated molecules recombine to reform the parent molecules.[34,46,47,60–63] For example, Vlček and coworkers observed population of trapping triplet states parallel to CO dissociation to decrease the quantum yield in $Cr(bpy)(CO)_4$ complex and decay of these trapping states within 8 ps and 87 ps.[47] However, in solution the reacting molecules are surrounded by the solvent molecules and therefore one should consider geminate recombination as a mechanism that decreases the quantum yield. The dissociated CO, containing a large amount of kinetic energy, collides with the wall provided by the first solvent shell and bounces back, which greatly increases the probability for recombination. Poliakoff and coworkers studied photochemistry of metal carbonyls at low temperature rare gas matrices.[64] They suggest that after dissociation of a CO group metal pentacarbonyl species undergo rearrangement. Depending whether in the final orientation the vacancy points towards the dissociated CO group or towards a matrix atom the five-coordinated species will recombine with CO or react with a matrix atom to form a solvated complex, for example $Cr(CO)_5$—Ar. According to their results the mechanism of the ligand substitution reaction in solution may follow a similar route. However, if the CO is able to escape from the solvent cage beyond the contact distance recombination becomes very unlikely.[34,65] On the other hand, after the solvation is complete, the open position in the coordination sphere of the metal center is occupied by a solvent molecule, and CO recombination is not possible anymore. Therefore, if geminate recombination is the mechanism that decreases the quantum yield of the reaction it should be fast. Harris and coworkers gave the upper limit of ~150 fs for recombination.[33] In transient absorption experiment it might be difficult to separate these processes because they often have a similar effect to the signal.

The UV excitation brings much more energy to the system that is needed to break a metal-CO bond. Typically the metal-CO bond dissociation energies are 150-200 kJ/mol (Mn-CO 150 kJ/mol,[60] Ru-CO 175 kJ/mol[39] or W-CO 192 kJ/mol[59]) while the UV excitation typically contains twice as much energy, for example 320 nm corresponds to 372 kJ/mol. In solution this excess energy is not consumed in dissociation of further CO ligands but

it is dissipated to the environment. So after excitation both the newly born product and the recovered parent molecules are vibrationally hot. Vibrational energy redistribution from the hot species to the solvent takes place from few tens of ps to few hundreds of ps.[33,60,63,66–68] In many cases experimentally observed biexponential relaxation kinetics are assigned to cooling of CO stretching mode and the low frequency modes coupled to it.[32,33,60,66,67,69] Owrutsky and coworkers also observed that the vibrational energy relaxation rate depends more on the type of vibrational modes of the complex excited than on the solvent or the amount of excess energy.[67] There is evidence from the experiments and from the quantum chemical calculations that the five-coordinated dissociation intermediate is born on an excited electronic state.[24,25,70] It is not, however, clear whether the solvated product is initially on the ground state or on the excited state. Only long relaxation times (hundreds of ps) suggest that electronically excited states may be involved in the relaxation process.

Chapter 2

Experimental

The purpose of this chapter is to describe briefly the sample preparation and analysis as well as the experimental technique, transient absorption spectroscopy, utilized in the work. References[71–73] provide more detailed description on the laser systems and experimental methods.

2.1 Sample Preparation and Characterization

In this study the light induced ligand exchange reaction of a ruthenium carbonyl complex was studied in solution. The sample molecule was synthetized in the University of Joensuu as a part of a synthesis series of halogen substituted ruthenium monobipyridyls. This study mainly focuses on the iodine substituted species (*trans*-I)Ru(dcbpy)$(CO)_2I_2$. The details of synthesis and characterization of the complex are described in paper I. The structure of the complex was determined by X-ray crystallography and NMR spectroscopy.

To prepare the product molecule in solution the complex was illuminated with a tungsten lamp. The crystal structure of the product molecule is not known but ^{1}H NMR spectrum of the aromatic protons was measured. By comparing the NMR spectrum with the NMR spectrum of the corresponding complex Ru(bpy)(CO)(Sol)Cl_2 (sol refers to a solvent molecule) whose crystal structure was known it is possible to deduce the structure of the product molecule to be (*cis*-I)Ru(dcbpy)(CO)(Sol)I_2.[74] In this study the solvent was either ethanol or acetonitrile.

To be able to obtain detailed understanding the electronic states of the complexes computational methods were used. Geometry of the reactant (in C_{2v}

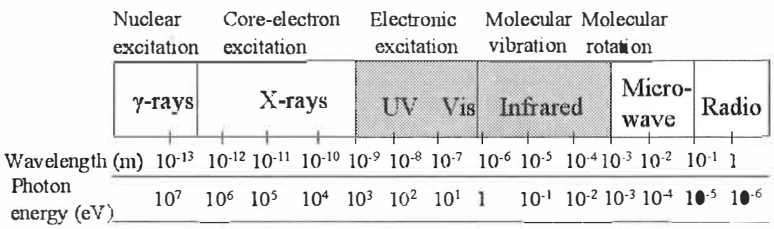

Figure 2.1: Regions of the electromagnetic spectrum and excitations taking place in different regions[80]

symmetry) and the product (C_1 symmetry) molecules were optimized by using a non-local hybrid density functional method B3PW91 and the Gaussian 98 program.[75] A standard double zeta basis set 6-31G* was used for all other elements except ruthenium and iodine, for which Huzinaga's extra basis[76](433321/4331/421) and (433321/43321/431), respectively, were used. Absorption spectra of the optimized molecules were calculated by using the intermediate neglect of differential overlap method parameterized for spectroscopy (INDO/S) at configuration interaction (CI) level of theory.[77–79]

2.2 Steady State Spectroscopy

Steady state spectroscopy is a standard method to get first glance information of the states of the studied molecules. Figure 2.1 shows different regions of the electromagnetic spectrum and the types of excitation that occurs in the regions. In this work measurements were carried out in the ultraviolet and the visible spectral regions and in the infrared spectral region. Measurement of UV/VIS absorption spectrum gives information on the electronic excitations taking place in the molecule. Knowledge of the electronic states is needed for interpretation of the excited state dynamics. Steady state IR spectroscopy provides information on the vibrational states of the molecules. Because vibrations of a molecule are related to certain nuclear movements, such as bond stretching or angle bending, IR spectrum provides information on the local structure of the molecule. For example functional groups like carbonyl, hydroxyl or cyano show characteristic IR absorptions. In this study the most interesting region in the IR spectrum is the carbonyl stretching region, where structural differencies between the reactant and the product molecules are clearly seen.

In principle the static absorption spectrum contains also dynamical information since wavelength and time are related via Fourier transform. In the simplest case Fourier transform of a time-correlation function (autocorrelation) of a laser pulse gives the spectrum of the pulse. In principle, similarly an absorption spectrum of a molecule contains the dynamic information of the system.[81] If excitation takes place to a bound excited state it is possible to deduce the lifetime of the excited state from the width of the corresponding spectral line if the line is homogeneously broadened. In principle the broadest line width in the absorption spectrum gives the shortest life time. However, in practice absorptions rising from different electronic and vibrational states may overlap, resolution of the spectrum may be insufficient and often line broadening mechanisms are unknown. Therefore, the underlying dynamics of the molecular system can not be extracted from the static absorption spectrum and time resolved spectroscopic methods have to be used in order to gain dynamic information on the studied system.

2.3 Transient Absorption Spectroscopy

Transient absorption spectroscopy was the main spectroscopic technique used in this study. It is a method which allows monitoring the dynamics of extremely fast events in real time. Figure 2.2 shows time scales and some typical events that are observable in the time range of tens of fs to few ns, which is roughly the time range of transient absorption measurements. Study of such fast events in real time is possible because the time resolution of the experiment is determined by the laser pulse duration. Today it is possible routinely to produce pulses as short as 4 fs which, for example, allow observation of wavepacket oscillations on the potential surface. The principle of the transient absorption experiment is rather simple. At the minimum two pulses from the same laser source are needed. An intense pulse, called the pump pulse, perturbs the system. This perturbation may lead to energy or electron redistribution inside the molecule or may initiate a reaction such as isomerization or dissociation. Then the second pulse, called a probe pulse, passes the sample and the intensity of the probe is monitored as a function of time delay with respect to the pump pulse. As the absorption spectrum of the sample is a signature of the species present in the sample, modifications in the absorption of the sample after the excitation, i.e. after the pump pulse, reflect pump pulse induced changes in the sample. The absorption of the sample may increase or it may decrease or completely new absorptions may be born indicating formation of a photochemical products. By changing

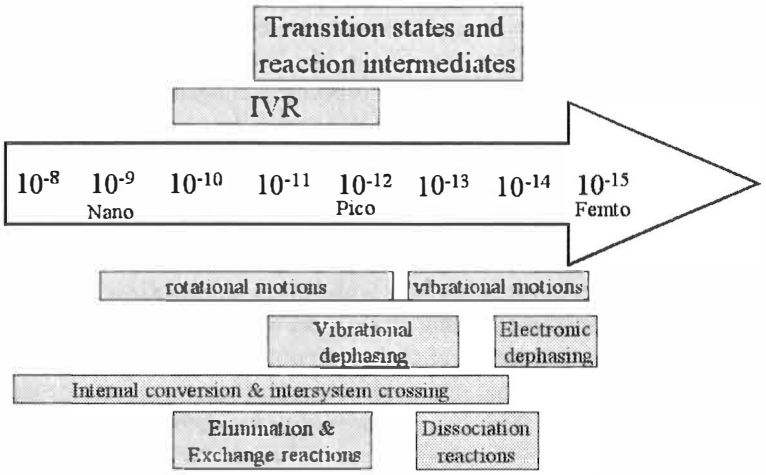

Figure 2.2: Time scale of various chemical and physical events taking place in the studied system[82]

the time delay between the pump and the probe it is possible to follow temporal behavior of these spectral features. The time difference between the two pulses is generated by varying their path lengths before the sample (see Fig 2.3). The pulses travel at the speed of light and one may then calculate that 10 fs time difference between the pulses corresponds to 3 μm difference in path.

The detected signal in the transient absorption measurement is the change in absorption, $\Delta A(\omega, \Delta t)$. This means that difference in absorption with and without pump pulse is measured as a function of frequency (ω) or time (Δt). After excitation of a sample with appropriate wavelength one can follow population dynamics at the given wavelength by varying Δt with time resolution determined by the pulse duration. On the other hand, one may measure the transient spectrum of the sample at the given time delay after the excitation pulse. Measurement of the transient spectrum may be helpful in assignment of different absorbing species. In both cases one has to know the spectral characteristics of the studied molecule, which can be obtained

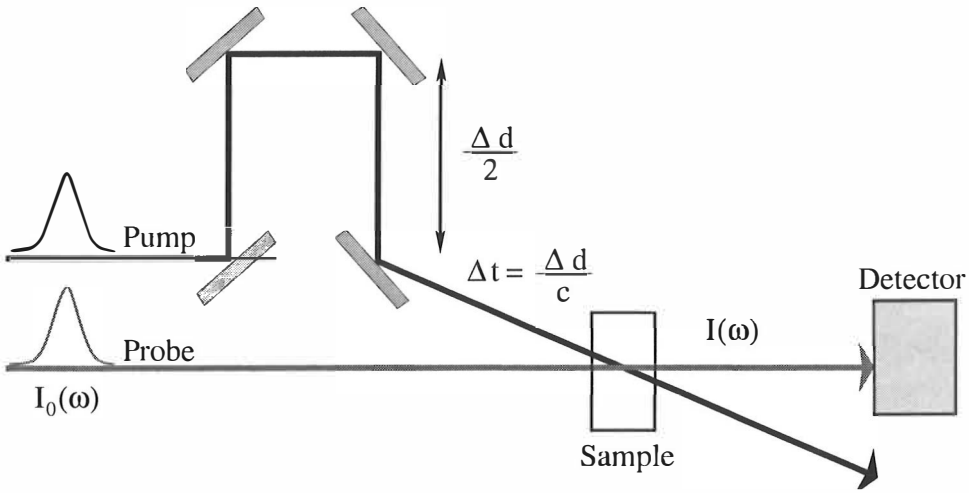

Figure 2.3: Schematic presentation of the pump and probe experiment

for example from a steady state spectrum.

2.3.1 Femtosecond Spectrometers

One of the most important components of a femtosecond spectrometer is a laser oscillator producing pulses. Nowadays modelocked Ti:sapphire oscillators are the most used for such purposes, and were also used in all experimental setups of this work. The repetition rate of Ti:sapphire oscillator is typically high (80 MHz), the pulse energy low (1-6 nJ) and the central wavelength is around 800 nm. Duration of the pulse of a Ti:sapphire oscillator is typically 100-150 fs but pulses as short as 5 fs have been produced.[72] In many cases the wavelength range of the Ti:Sapphire oscillator is not suitable for the experiment and its wavelength needs to be tuned. There are several techniques based on non-linear optics to do that but in general higher pulse energies and lower repetition rates for the experiments are needed. Therefore, Ti:sapphire oscillator is usually connected to Ti:sapphire amplifier, which amplifies the seed pulse generated by the oscillator and decreases the repetition rate typically to 1-10 kHz. There are basically two types of amplifiers, which are used in this work: regenerative amplifiers, multipass amplifiers or their combination. Before amplification seed pulses from the

oscillator needs to be stretched in time because otherwise amplifier optics would be damaged. After amplification pulses are compressed roughly to their initial duration. The pulse energies of the amplified pulses vary from hundreds of microjoules to few millijoules.

There are a variety of techniques that can be used to tune the wavelength of the amplified laser beam. One of the simplest methods is harmonic generation. In this work second harmonic generation (SHG) in a BBO crystal was used to produce pump pulses. In this nonlinear process two photons initially having the same frequency propagate trough a suitable nonlinear material, mix and give rise to a photon with twice the original frequency. Efficient frequency doubling can only take place in so called birefringent crystals where different polarization components propagate with different speeds depending on the relative orientations of the initial beam and the main optical axis of the crystal. In order to find the SHG signal certain phasematching conditions must be fulfilled. This can be achieved by turning the angle of the crystal, with respect to the incoming beams.

Another possibility to change the frequency of the fundamental laser around the visible and near-IR regions is white light continuum generation. Focusing a small fraction ($\sim 1\mu$J) of the amplified laser beam carefully on a sapphire plate leads to self focusing of the beam in a transparent medium and generation of single filament white light continuum around the fundamental frequency. Most of the pulse energy is centered around the fundamental frequency but a flat intensity distribution of the light generated covers the wavelength region from 450 nm to 700 nm and an equally wide wavelength range in the IR side of the fundamental frequency. Due to its weak intensity the white light continuum is suitable for probing purposes. During propagation in the transparent medium the red wavelengths of the pulse travel faster than the blue wavelengths. This phenomenon is called group velocity dispersion. A pulse where the red wavelengths are in the leading edge of the pulse and the blue wavelengths in the trailing edge is said to be chirped. The white light continuum is typically strongly chirped due to strong dispersion of the sapphire crystal and the collimating optics. Therefore, in pump and probe experiments where the white light continuum is used as a probe the time zero varies from one wavelength to another and must be corrected if for example transient spectra are measured.

If two photons with different frequencies enter a suitable birefringent crystal the two photons are mixed and new frequencies may be generated. Mixing of two photons and generation of new frequencies are called parametric

interactions. Parametric processes utilized in this work were parametric amplification, sum frequency generation and difference frequency generation. Noncollinear optical parametric amplification (NOPA) is today widely used for producing ultrashort laserpulses in the visible and in the near-IR region.[83–85] In a OPA a weak signal pulse (angular frequency ω_1) interacts with a strong pump pulse (angular frequency ω_2) generating a new frequency $\omega_3 = \omega_2 - \omega_1$ called idler and amplifying the weak signal pulse at angular frequency ω_1. The amplified signal can be then used to pump the sample, used as a probe pulse or in the generation of new frequencies via other parametric interactions. In an optical parametric amplifier (OPA) the white light continuum seed (signal) pulses are overlapped in time and space with intense pump pulses of fundamental beam. Nowadays often OPAs with a noncollinear phase-matching geometry and frequency doubled fundamental pulses (400 nm) for pumping are used. An advantage of 400 nm pumped NOPA is that it is possible to amplify spectrally broad bandwidths of the white light continuum with high gain.[86] The output pulses from a NOPA are chirped but they can be compressed by using a prism pair or chirped mirrors all the way down to 4 fs. Considering the relationship between duration of the pulse and spectral width, the wider the amplified bandwidth the shorter the pulse duration after compression.

Most of the molecules, like the present ruthenium complex, have intense absorption bands in the UV region. To be able to effectively excite these transitions UV wavelengths must be generated. In this work UV wavelengths were produced by sum frequency generation. In this parametric process one intense photon of the fundamental laser frequency (ω_2, 800 nm) was combined with an output from a NOPA (ω_1, 530 nm) to produce an UV photon (ω_3, 320 nm).[87] In many cases probing of the vibrations in the IR region gives structurally more specific information on the studied molecules than the probing of the electronic transitions in the visible region. Transient UV-pump-IR-probe spectroscopy is an ideal method to study reactive systems since IR detection gives direct bond specific information as well as information on the vibronic states of the molecules. Therefore, the appearance, intensity change, spectral shift or disappearance of a vibrational mode during the experiment is a direct indication of rearrangement of the nuclear coordinates. Generation of femtosecond IR pulses is complicated and also a new technique, since only in the end of 90's a method of generating stable fs mid-IR pulses was reported.[88] In this work, femtosecond mid-IR pulses were produced by mixing of the signal and the idler from the second amplification stage of an OPA in $AgGaS_2$ crystal. This method generates difference frequencies around 2000 cm^{-1} ($= 5\ \mu m$), which were then used for probing.[89]

Figure 2.4 shows the simplified transient absorption setup. Pulses are generated by an amplified Ti:sapphire laser system. For the experiments the pump pulses were generated either in a NOPA with subsequent sum frequency generation (papers III and IV) or directly frequency doubling the fundamental laser frequency (paper II). The probe pulses were taken from white light continuum generation (VIS, paper II), from NOPA (short VIS, paper IV) or from NOPA followed by frequency difference mixing (IR, paper III). The pump pulses travelled via a variable delay line. By changing the position of the mirror on the delay line it was possible to vary the time difference of the pump and the probe pulses at the sample.

Another important component of the setup is a mechanical chopper. By chopping the pump beam the signal with and without pump is alternatively detected, from where the absorption changes may be calculated. The pump and the probe were focused to the same spot to give an overlap in space inside the sample. After the sample the probe wavelength was selected with interference filter or monochromator/spectrograph and detected either with photodiodes with digitizing electronics (paper II), a diode-array (paper III) or a lock-in amplifier and a diode (paper IV). To decrease experimental noise in some cases also a third pulse called the reference pulse is used. The reference pulse is identical to the probe with an exception that it does not overlap with the pump pulse. By using the reference pulse it is possible to remove noise due to ambient light, electronics, laser fluctuations or emission from the sample. The transient absorption signal was calculated as:

$$\Delta OD(\nu, \Delta t) = log(\frac{I_{probe}(\nu)}{I_{ref}(\nu)}) - log(\frac{I_{0,probe}(\nu)}{I_{0,ref}(\nu)}) \tag{2.1}$$

where $I_{probe}(\nu)$ and $I_{ref}(\nu)$ are intensities of the reference and probe beams with pump on and $I_{0,probe}$ and $I_{0,ref}$ intensities of the probe and reference beams with pump off, respectively.

2.3.2 Data Analysis and Assignments

As discussed before, a pump and probe experiment may be carried out either by recording the time evolution at a certain wavelength, called a kinetic measurement, or by measuring the transient absorption spectrum over a wavelength region at a specific delay between the pump and the probe pulses. The

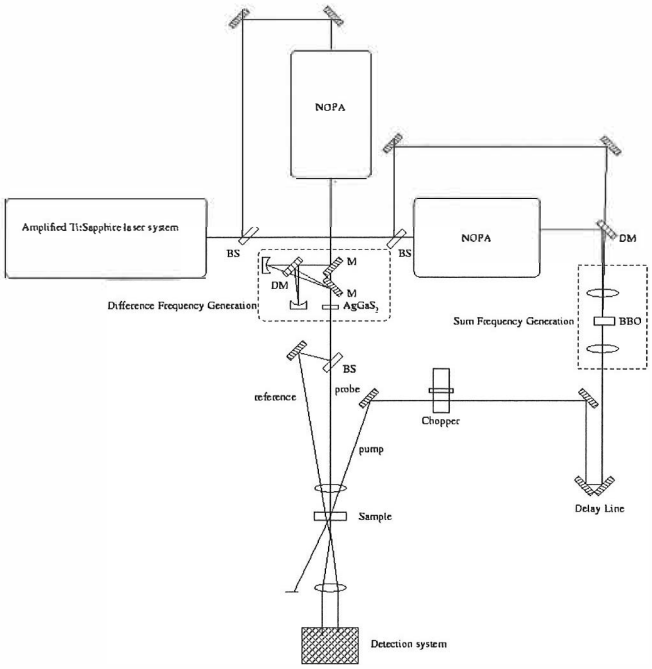

Figure 2.4: Simplified transient absorption setup. In this work frequency upconverted NOPA pulses (papers III and IV) or frequency doubled fundamental pulses (paper II, not in the figure) were used as pump. Probe pulses were taken from NOPA or OPA followed by difference frequency mixing of the signal and idler. It is also possible to use white light continuum as a probe (not included in the figure). In the figure BS refers to beamsplitter and DM to dielectric mirror. Components inside the dashed boxes are optional and were not in use for all of the experiments.

transient absorption spectrum is useful in assignment of the kinetic signals at different wavelengths while from kinetic traces it is possible to extract time constants for the rise and/or decay processes involved. It was assumed that the signal follows multiexponential decay kinetics:

$$I(t, \lambda_i) = \sum_{j=1}^{n} A_j(\lambda_i) \cdot exp(\frac{-t}{\tau_j}) \tag{2.2}$$

where n is the number of the kinetic components in the system and equals to number of chemical components or states of the system. In the fitting procedure least square fitting of a nonexponential decay was used. In determination of the sub-ps kinetics one should always remember that the observed signal is a convolution of the kinetics of the system and the instrumental response. Instrumental response, which is defined both by the laser pulse width and response of the detection system, may be determined as cross-correlation of the pump and the probe signals for example in a BBO crystal. Therefore, to be able to accurately determine the fastest components of the observed signal the data must be deconvoluted with the the instrumental response function. Other important function of the instrumental response is to determine the exact time zero of the signal, which has to be known when resolving fast rise components. It is possible to fit the recorded kinetics at different wavelengths separately. However, often kinetics, or lifetimes of the observed chemical events or states, at different wavelengths are connected to each other. For example a decay of an excited state absorption at one wavelength may be seen as formation of a new absorbing species at another wavelength. Thus it is often physically more relevant to use global fitting procedure instead of fitting of the individual traces. In global analysis the attempt is to find a single parameter set, which is capable of describing the data measured at all wavelengths. This often makes the assignment of the observed time constants easier.

The transient absorption signal may be either positive or negative depending whether transmittance of the sample is increased or decreased after excitation. Positive transient absorption signal means that the pump pulse creates new absorbing species in the sample. These might be either species absorbing from the excited states or an indication of formation of photoproducts. Negative absorption is either due to stimulated emission or ground state bleaching. Probe pulse may induce emission of a photon identical to the probe photon from the excited state to the ground state. Then the intensity of the probe pulse is increased, which is observed as negative transient absorption signal. After excitation the population in the ground state decreases and fewer pho-

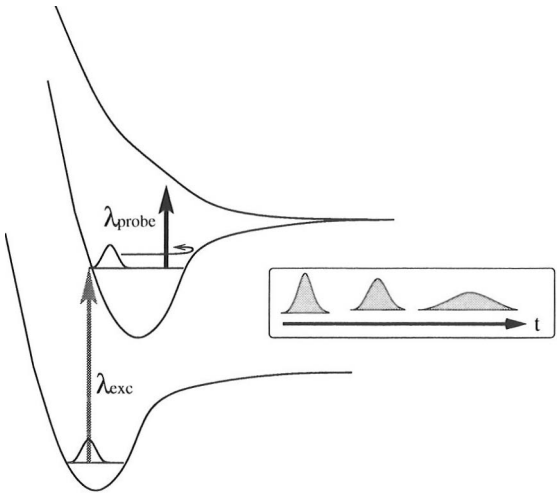

Figure 2.5: Birth of a wavepacket as a result of excitation on the potential surface. The second pulse excites the wavepacket to an upper dissociative surface. The inset shows its dephasing as a function of time.

tons of the probe pulse are absorbed into the sample and a negative transient absorption signal is observed.

When the pulse length is shorter than the decoherence time of the sample the observed kinetics may show some oscillations. A short light pulse in time domain is spectrally broad. Such an excitation pulse generates a wavepacket as a coherent superposition of (vibrational) states in the excited electronic state. The wavepacket starts to travel back and forth on the potential surface. Figure 2.5 shows simple potential surfaces where the motion of the wavepacket and its effect on the transient absorption signal is visualized. An excitation pulse prepares the wavepacket on the excited state potential surface in the Franck-Condon region. The second pulse probes a certain region of the potential surface. The wavepacket starts to move on the surface from its initial location and when it arrives to the probe window an increased absorption is observed. Absorption decreases when the wavepacket moves away from the window. Movement of the wavepacket can thus be seen as oscillations in transient absorption signal. The amplitude of the oscillations decays due to spreading of the wavepacket in time due to dephasing of the

excited vibrational modes. These oscillations may then be assigned to the vibrational modes of the molecule. The signal with oscillations may be fitted with similar multiexponential function as described previously with an additional component consisting of exponentially damping cosine functions. From the fit also the damping time of the oscillation may be determined. Other possibility is to Fourier transform the residual signal of the data after removing the exponential components. The Fourier transform then gives the frequencies of the oscillating modes.

Chapter 3

Results

This chapter presents the main experimental results of this work. In the thesis the mechanisms of a ligand exchange reaction of a Ru complex were resolved. This chapter follows the course of the work: we started with the characterization of the sample and its steady state spectroscopy. Then we moved on to study the electronic states of the reactant and the product complexes. Finally, the ongoing reaction was studied by using transient absorption spectroscopy.

3.1 Steady State Spectroscopy

In paper I synthesis and characterization of the (*trans*-I)Ru(dcbpy)$(CO)_2X_2$ where X is either Br or I are described (Figure 3.1) As the present work concentrates in determination of the reaction dynamics of the iodine analogue the time resolved results for the iodine complex only are presented. It was observed that a photoinduced reaction takes place in both mentioned complexes in solution. The reaction is observed as spectral changes in the visible and in the IR regions. The reactant molecule shows two intensive absorptions in the CO stretching region in acetonitrile: symmetrical CO stretch at 2002 cm^{-1} and an antisymmetrical one at 2058 cm^{-1}. During the illumination both parent molecule absorption bands disappear simultaneously together with formation of a new absorption in the CO stretching region around 1970 cm^{-1}.

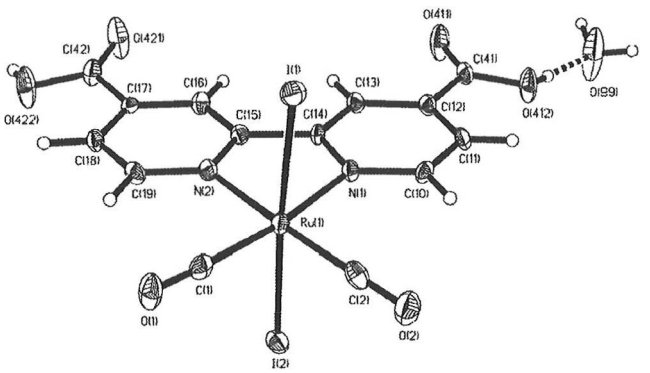

Figure 3.1: X-ray crystal structure of the reactant

In the visible spectral region the reactant molecule absorbs very weakly. In the UV region, however, the reactant molecule has two distinct absorption bands at at 320 nm and at 230 nm. The product molecule shows absorption also in the visible spectral region around 520-550 nm slightly depending on the solvent. By comparing the number of photoexcited molecules with the number of product molecules obtained in the reaction the quantum efficiency was estimated to be 0.3 at 458 nm excitation indicating that only 30 % of the initially excited molecules turn into the final product. In paper IV we studied quantum efficiency as a function of wavelength and observed that quantum yield increases when excitation wavelength decreases. By using NMR spectroscopy the structure of the product molecule was determined to be (*cis*-I)Ru(dcbpy)(CO)(Sol)I_2.

It was also observed that at lowered temperatures the parent molecule is luminescent but luminescence quenches rapidly with increasing temperature from 77 K to 116 K. The exponential fit of luminescence intensity *vs.* 1/T gave 10 kJ/mol for the activation energy for the process responsible for quenching of the emission. The emission maximum of the product is the same as that of the reactant emission at 652 nm in contrast to what is stated in paper I where there was an experimental error in the emission spectrum of the product. The emission intensity of the product is however much weaker than that of the reactant (see Fig. 3.2).

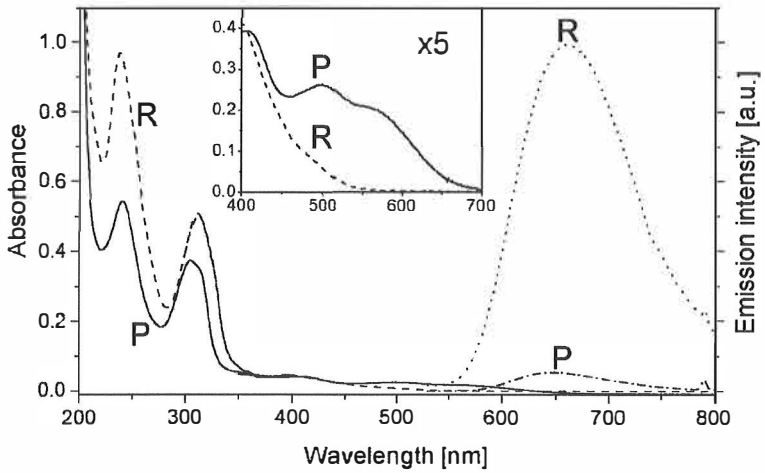

Figure 3.2: Absorption and emission spectra of the reactant and the product

3.2 Electronic States

To be able to understand the dynamics of the reaction we decided to study first the excited state properties of the reactant and the product separately. Therefore both quantum chemical calculations and transient absorption measurements of the reactant and the product were carried out in paper II.

Geometry optimization was carried out by using DFT calculations as explained in the experimental part. According to single point ZINDO/CI calculations three highest occupied molecular orbitals of the reactant have almost the same energies, and they contain contributions from ruthenium 4d and iodine 5p atomic orbitals (H, H-1). The H-2, H-3 and H-4 orbitals are almost pure iodine 5p atomic orbitals. The lowest unoccupied π^* molecular orbitals (L, L+2, L+3 and L+4) are localized on the dcbpy ligand (see Table 1 in Paper II). The L+1 molecular orbital is an exception: It is a mixed ruthenium-iodine orbital π^*(Ru-I). According to ZINDO/CI calculations the most of the lowest energy excitations are MLCT transitions or MC transitions although such classification may be too simplified since most of the metal orbitals are not pure Ru d orbitals but contain contributions also from iodine p orbitals. The transition at 320 nm is an exception being a $\pi^* \leftarrow \pi$

transition centered on dcbpy ligand.

The occupied molecular orbitals (from H to H-6) have strong contribution from iodine 5p and a smaller contribution from ruthenium 4d atomic orbitals π(Ru-I). The lowest unoccupied orbitals π^*(dcbpy) of the product molecule are localized on the bipyridyl ligand (see Table 1 in paper II). In the product molecule the lowest energy transitions may be described as π^*(dcbpy) $\leftarrow$ π(Ru-I) transitions. The calculated transition energies of the product are clearly smaller than the corresponding energies in the reactant and hence the absorption spectrum is predicted to be red shifted with respect to the spectrum of the reactant, in accordance with the experimental spectra (Fig. 3.2).

Transient absorption measurements for both complexes were carried out in the wavelength region from 460 to 825 nm. Broad excited state absorption dominates the spectra in the entire visible region. [Ru(dcbpy)$(CO)_2I_2$] exhibits two transient absorption bands one peaking at 480 nm and the other at 570 nm. The signal shows a rise time of (4.1$\pm$0.5) ps at 480 nm and a decay of the excited state absorption at 570 nm with a similar time constant. An isobestic point at 495 nm indicates that the two processes are related. After initial relaxation the excited state absorption over the whole visible region decays in ns time scale. The ns-process is assigned to ground state recovery. Excited state kinetics was independent of temperature from 77 K to 150 K.

The transient spectrum of the product shows strong excited state absorption extending far towards the red. Kinetics of this absorption proved to be dependent on temperature and solvent. In solid ethanol at 700 nm probe wavelength a fast initial ps decay and a long decay component of 400 ps was observed. At room temperature the corresponding decay contains a fast ps component but the rest of the signal decays in $\sim$20 ps. The product molecule with an acetonitrile ligand at room temperature showed, besides the fast ps decay, also the long decay component of $\sim$400 ps, observed in ethanol only at 77 K. Neither temperature nor the solvent affects the kinetics in the blue part of the spectrum.

3.3 Reaction

Kinetics of the ongoing reaction were measured in the visible region as well as in the mid-IR region with a time resolution of $\sim$ 170 fs. It turned out that this time scale is not sufficient to resolve the early dynamics of the reaction

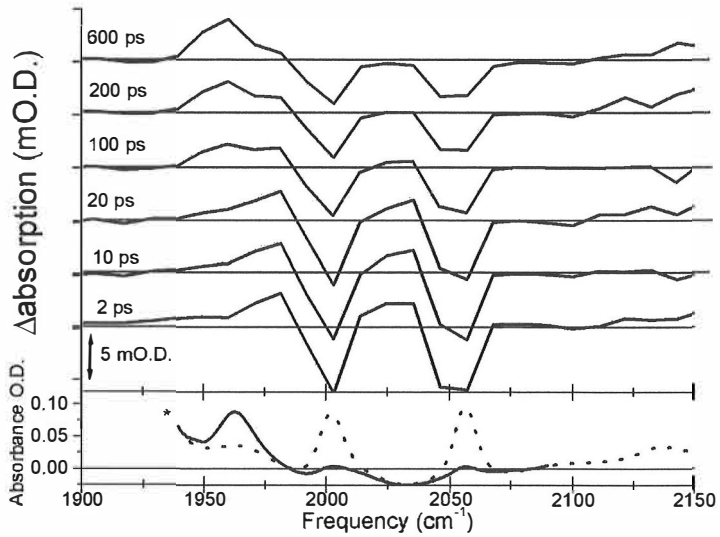

Figure 3.3: Transient IR spectra of the reaction solution as a function of time. The lowest panel shows steady state IR spectrum of the parent (dashed line) and the product (solid line) in ethanol, respectively. The steady state spectra are not shown below the asterisk (1940 cm^{-1}) due to strong absorption of the solvent.

and hence kinetics were measured also with $\sim$ 20 fs time resolution in the visible spectral region.

Transient IR spectroscopy was used to study the time evolution of absorptions in the CO stretching region after UV excitation (Fig. 3.3). Transient IR measurements were carried out using both parallel and perpendicular polarizations between the UV-pump and the IR probe. After initial excitation the parent molecule bleach signals excitation at 2003 cm^{-1} and 2057 cm^{-1} and also formation of induced absorption on the red side of the bleach bands at 2024 cm^{-1} and 1980 cm^{-1} is seen within time resolution of the experiment. The induced absorption signals decays with the same time constants of 4 ps and 70 ps as the parent molecule bleach signals recover. An induced absorption signal is seen around 1962 cm^{-1}. Formation of the absorption is limited by the instrumental response time and in the picosecond time scale the narrowing of the absorption is observed with time constants of 18 ps and 270 ps.

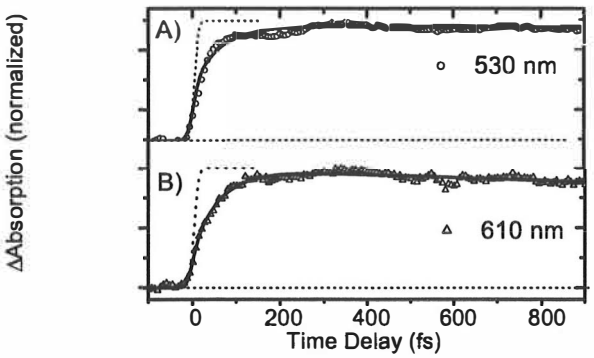

Figure 3.4: Rise of a transient absorption signal at 530 nm and at 610 nm, respectively. The signal is very similar at all wavelengths showing a rise component with 62 fs time constant and a low frequency oscillating component.

We have also measured the transient absorption spectrum of the complex in solution in the visible spectral region in different alcohol solutions with exciting the solution at 400 nm. The problem with the interpretation of the data collected in the visible region is that the induced absorptions arising from the parent molecule and the CO dissociation product overlap. The transient absorption signal remains positive at the wavelengths, where the ground state product absorbs, while in the low energy side of this absorption the signal decays to zero. This observation is interpreted as an indication of formation of a stable photoproduct of the reaction. According to the results in the ps timescale kinetics seem to be independent on the alcohol solvent. In principle the same information about the system can be extracted from the measurements also in the IR region. In fact, it turned out that the decay of the transient absorption signal is very similar in the IR and in the visible, and it is possible to fit the data by using the same kinetic constants of 4.3 ps, 70 ps and 270 ps. In the visible region it is not possible to spectrally separate the reactant and the product absorptions. The red end of the spectrum seems to be an exception since there 270 ps relaxation component of the product was not observed.

At the early delays after the UV excitation transient absorption signal of the ongoing reaction shows an increased absorption at all studied probe wavelengths from 510 nm to 650 nm with almost similar kinetics independent of wavelength(Fig 3.4). Approximately 50 % of the rise of the signal occurs

within the pulse and the rest of the signal rises exponentially with a time constant of (62±5) fs. In addition signals show oscillatory components (Fig. 3.5). The lowest frequency oscillation (90±5 cm^{-1}) is present at all probe wavelengths. Around 570 nm also three other frequencies, (378±20 cm^{-1}), 514±20 cm^{-1}) and (871 ±50cm^{-1}), are present. Damping of the oscillations occurs in 500fs (90 cm^{-1}), 45 fs (378 cm^{-1} and 514 cm^{-1}) and 30 fs (871 cm^{-1}).

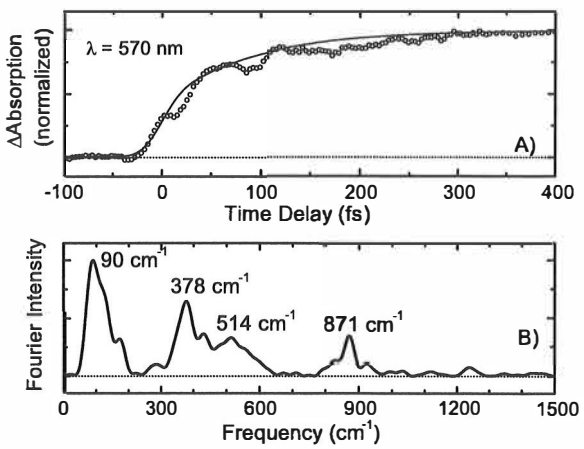

Figure 3.5: Upper panel: The rise kinetics of the signal at 570 nm. Lower panel: Fourier transform of the residual signal (the data minus the fit) shows three oscillating components: 871 cm^{-1}, 514 cm^{-1}, 378 $^{-1}$ and 78 cm^{-1}.

Chapter 4

Discussion

The purpose of this chapter is to clarify and explain the ideas that lead us to the suggested mechanism of the ligand exchange reaction. Also the observed time constants are assigned to the different steps of the reaction.

4.1 Structure of the Product

In principle, there are several possible structures of the product depending on whether the remaining ligands are reorganized after CO dissociation and what is the mechanism of the reorganization. The Berry pseudorotation has been used to explain the ligand reorganization in metal hexacarbonyls $M(CO)_6$.[25] It is a very widely accepted mechanism that explains the structural nonrigidity of five-coordinated main group elements.[49] In the pseudorotation the reaction coordinate is simultaneous bending of two axial and two equatorial ligands and it leads to exchange of the position the two axial ligands with the equatorial ones. In the present complex, however, such mechanism is not possible because bipyridyl ligand fixes positions of two equatorial site and the square pyramid may not be formed as in $M(CO)_6$ complexes.

Figure 4.1 shows all the possible configurations of the product species and the calculated energies for possible transformations between the species. Structure of the parent molecule is known from X-ray crystallography. The parent molecule has two equal CO groups in the equatorial positions of the ligand sphere. In paper I the structure of the product was studied experimentally and ^{1}H NMR of the bipyridine region suggest that the product molecule has

different ligands in the axial positions. Moreover, the NMR spectrum was compared to the NMR of the similar complex with chlorine ligands instead of iodines, whose crystal structure was known.[74] The spectrum clearly indicates that the structure of the product is Ru(dcbpy)(CO)(Sol)I_2, where sol is a solvent molecule. The structures and energetics of the ligand exchange reaction was studied by computational methods (paper IV). Dissociation of one of the CO groups of the parent molecule requires 175 kJ/mol of energy. According to the calculations the reorganization of the remaining ligands of the five-coordinated intermediate also requires energy. The attachment of a solvent is a spontaneous process releasing energy but the overall reaction is endothermic indicating that the reactant is energetically more favorable than the product. However, one must remember that the calculation does not take into account the solvent environment which may stabilize the five-coordinated intermediates and may favor reorganization of the ligands. On the other hand, the energy differences correspond to ground state structure. Most probably the five-coordinated intermediate is its excited state where the conformation change may be (nearly) barrierless process.

4.2 Model for the Ligand Exchange Reaction

From the structures of the product and the reactant it is possible to draw some conclusions of the different steps of the reaction. One would expect to see dissociation, change of the position of an iodine ligand and coordination of the solvent. Moreover in paper I the quantum yield of the reaction has been determined to be 0.3 after 458 nm indicating that 70% of the excited parent molecule turn back to the reactant ground state. To understand better the non-unity quantum yield we also studied its wavelength dependence (paper IV). In fact it turned out that the quantum efficiency depends on the excitation wavelength and increases with increasing excitation energy. Several models can be used to explain the non-unity quantum yield. In the simplest model the dissociation reaction involves direct population of the dissociative potential energy surface. Then, due to a cage-effect provided by the solvent the CO is recombined with the five coordinated intermediate and a hot parent molecule is reformed in the electronic ground or the excited state. On the other hand, if the initially prepared state is bound, the mechanism may involve competing channels of relaxation of the excitation: dissociation and internal conversion or intersystem crossing to lower lying states.[24,46,61]

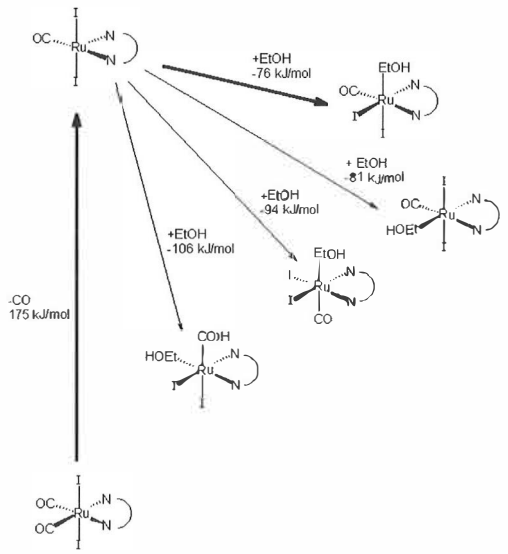

Figure 4.1: Schematic presentation of the calculated energies of possible reaction steps. The thick solid line shows the most probable reaction route according to experimental observations

It was observed that in frozen environment, in ethanol glass at 77 K, the overall reaction is prevented (papers I and II). However, most probably a frozen environment does not prevent the population of the dissociative state. This means that while probing the kinetics of the frozen reactant solution we observe kinetics related to recovered parent molecules. In the frozen environment a great majority of molecules that ended up on a repulsive surface should undergo geminate recombination since no final product was observed. The excited states at lowered temperatures live nanoseconds indicating that triplet states play a role in relaxation process of the recovered parent molecules. Also long lived luminescence that was strongly red shifted compared to absorption spectrum was observed giving another indication of the triplet state involvement in the relaxation. In other ruthenium complexes it has been observed that the intersystem crossing may be very fast, occuring on the sub-100 fs timescale.[90–92] It is not clear from the present data whether the intersystem crossing takes place before dissociation or after recombination. In the transient IR measurements it is possible to selectively probe the recovery of the parent molecules. In these measurements the observed recovery times were of the order of tens of ps. Because the recovery of the ground state absorption in the transient IR measurements is an order of magnitude faster than the lifetime of the excited state of the reactant at 77 K it is possible that the intersystem crossing takes place only after dissociation. However, straightforward comparison of the measurements carried out at the room temperature and at 77 K may be misleading because relaxation routes may involve some thermally activated processes.

In the transient IR experiment only ~15% recovery of the bleach signal was observed (paper III). It gives an upper limit of 55 % for reaction quantum yield at 320 nm. If the quantum yield is lower than that it may indicate that part of the parent molecules recover faster than time resolution of the experiment. Immediately after excitation the transient spectrum shows induced absorptions on the red side of the parent molecule transitions at 2024 cm^{-1} and 1980 cm^{-1}(Fig. 3.3). These bands are assigned to excited state absorption of the hot parent molecule and are redshifted by ~ 20-30 cm^{-1} due to anharmonicity.[59,67] The instrument response time limited rise of the absorption at 2014 cm^{-1} is an indication of the sub-ps recovery of the hot parent molecules. This sort of behavior may be observed because the majority of the excited molecules undergo ultrafast internal conversion to hot ground state and only a smaller fraction dissociates. On the other hand, if all molecules dissociate but a fraction of them undergoes geminate recombination ending up on an electronic ground state on sub-200 fs time scale, a similar signal should be seen. Therefore, the time resolution of the experiment does not

allow us to distinguish whether the recovery is due to internal conversion, geminate recombination or both. In any case it actually indicates that most probably the quantum yield for the reaction is less than maximum value of 55 % as suggested by the parent molecule bleach recovery.

Let us then move on to discuss the mechanism of the dissociation reaction itself. The quantum chemical calculations suggest that the excitation at 320 nm promotes an electron from a π orbital of the dcbpy ligand to a π^* orbital of the same ligand (see paper II). It is reasonable to assume that the initially excited state is not a repulsive state with regard to CO dissociation since it does not involve either orbitals of the metal or the CO ligand. This implies that predissociation (internal conversion to a repulsive state) takes place prior to dissociation. According to literature the repulsive state may be either a LF state or a MLCT state.[24,25,93] Furthermore, according to calculations these states are often very strongly repulsive leading to fast dissociation of a CO group. In the transient absorption signal one would expect to observe the dissociation of a CO as an increase of an absorption since a new absorbing species is born. On the other hand, also other processes than dissociation may lead to increased absorption of the system. Absorption from lower energy excited state after internal conversion from the initially excited state to a lower energy bound state or internal conversion to a triplet may also contribute to the rise of the signal.

In the experiments carried out with 20 fs time resolution (paper IV) we, indeed, observed a rise component with $\sim$ 62 fs time constant at all probe wavelengths from 510 nm to 650 nm. We assign this rise component to the formation of a five-coordinated intermediate and we consider the intermediate to have been formed when the CO group has escaped the first solvation cage. Thus after ending up to a dissociative potential surface a fraction of the molecules collide with the potential created by the solvation shell and undergo very fast geminate recombination to reform the parent molecules. The geminate recombination was not observed in our transient absorption signal in the visible region; we only know the upper limit of 170 fs from the transient IR measurements. On the other hand, it is possible that the observed time constant of 62 fs is a sum of two competing processes, dissociation and recombination. Time constant for dissociation then depends on branching ratio between the two processes. For example, if the recombination would be the only process that decreases the quantum yield, the time constant for dissociation would be 154 fs assuming 0.4/0.6 branching for dissociation/recombination. In any case, the dissociation is faster than IVR, since from the transient IR measurements it is known that the timescale for IVR of the present complexes is order of tens of ps and also, the IR measure-

ments give the upper limit of 170 fs for dissociation. This means that IVR is restricted to the modes near the reaction coordinate and the timescale does not allow a complete statistical redistribution in the phase space of the reaction.[94,95] In fact, the fast dissociation time constant indicates that initially after excitation a great deal of excess energy must be concerted to kinetic energy of the dissociating CO group. If all excess energy would turn into kinetic energy the maximum speed of the dissociating component would be 0.037 Å/fs which in accordance with the maximum recoil velocity of 0.042 Å/fs for dissociating CO group of $Mn_2(CO)_{10}$.[29] Hence, within 62 fs the CO fragment travels 2.3 Å which is roughly twice the initial bond length. However, it is likely that all excess energy is not converted to kinetic energy of the CO group leading to a smaller recoil velocity and separation of the species after the time period of dissociation. Also the observation oscillations in the transient absorption signal supports the assumption that a fraction of the excess energy is distributed to vibrational modes of the reacting species.

Next we will have a closer look on the oscillatory features observed in the transient absorption signal in the visible spectral region. A short excitation pulse creates a vibrational wavepacket, which is a coherent superposition of the vibrational states of an electronic state. The wavepacket starts to move on the potential surface and thus the second pulse probes the position of the wavepacket on the potential surface. If the difference between the excited state and the final state of the probe process is not constant the motion of the wavepacket is seen as periodic modulation of the transient absorption signal. Wavepacket dynamics was initially observed in isolated molecules on I_2 and Na_2[23,96,97] but since oscillations have been observed in bigger and even in reactive systems.[98–102] Within time the wavepacket broadens as the probe samples a large area of potential energy surface and the coherent oscillations disappear. Therefore, observation of coherent features in the signal is an indication of well defined and slowly dephasing wavepacket. The present data shows four oscillating components: a low frequency component of 90 cm^{-1} present at all wavelengths and three high frequency components at 378 cm^{-1}, 514 cm^{-1} and 871 cm^{-1} around 570 nm. Due their different wavelength behaviour the high and low frequency oscillations most probably are related to different states/absorbing species. It was observed that the low frequency oscillation is independent on the initially excited state (see paper IV). A period of the lowest frequency oscillation is so long (370 fs) that it must be related to the five-coordinated intermediate. This means that the low frequency vibration is excited by CO dissociation. Intuitively the excited mode that is in charge of the conformational change of the intermediate is the I-Ru-I bending mode or Ru-I stretching mode . This assumption is

also supported by our quantum chemical calculations (paper IV) and is in accordance with pseudorotation mechanism observed for metal hexacarbonyls previously.[24,25] In paper III we measured the kinetics of the reaction in different alcohol solutions. No dependence of the kinetics on the chain length of an alcohol was observed in the ps time scale. From those measurements one then may conclude that attachment of a solvent molecule occurs in sub-ps timescale. Therefore, we suggest that exponential damping time of the low frequency oscillation with time constant of 500 fs is due to a solvent molecule coordination to the opened axial site simultaneously with the change of orientation of the iodine from the axial site to equatorial site. Within this time scale also other processes, such as collisions with solvent molecules, operating parallel to solvent coordination may cause damping of oscillation.

The high frequency oscillations of 378 cm^{-1}, 514 cm^{-1} and 871 cm^{-1} are observed only in the narrow wavelength region around 570 nm. The initially excited π^* state of the bipyridyl ligand state is a bound state and a broad-band UV excitation pulse creates a coherent vibrational wavepacket on this state. Assuming to a first approximation that the excited state absorption band is being frequency shifted by the active vibrations, the resulting spectral oscillations should scale as $d\alpha/dn\nu$, α representing the absorption cross section and ν the probing photon frequency. We then assume that the high frequency oscillations of the wavepacket are most clearly seen around the inflection point of the reactant excited state absorption, occurring around 570 nm. According to calculations around 378 cm^{-1}, 514 cm−1 and 871 cm^{-1} several modes that involve dcbpy ring deformations of the intermediate are present. Damping of these oscillations is too fast (40 fs and 30 fs) to be assigned to intramolecular vibrational redistribution of energy but damping more likely results from IC to another electronic state. Hence, we assign the high frequency components to the initially excited bound state and damping of the oscillations to IC to a lower lying electronic state. Considering the wavelength dependence of the reaction quantum yield it is possible that branching of the population of the initially excited state takes place. This means that the observed time constant of 30 fs of damping of the oscillations is a sum of parallel processes of population of dissociative state and lower lying bound state. Then, the lower is the excitation energy the bigger fraction of the excited molecules undergo IC to a lower lying (excited) state and the smaller fraction end up a repulsive potential surface. It is also possible that the increase of excess energy increases also the probability of dissociation with respect to recombination as the mean kinetic energy of the leaving group may increase. The time constants for these processes are dependent on the branching ratios at the different steps of the reaction and since the

kinetic constants observed are, most probably, sum of these processes we are not able to unambigiously resolve.

Chapter 5

Conclusions

Transient absorption is a quite complex technique. Not only the experimental setup is complicated but also the results are often difficult to interpret. By varying the experimental parameters such as excitation and probe wavelengths and with the help of quantum chemical calculations we were able to create a model for the ligand exchange reaction of $Ru(dcbpy)(CO)_2I_2$. Probing of the kinetics in the mid-IR region is a very elegant method to study reacting systems because it gives direct information on the structural changes in the molecule. Unfortunately the time resolution available for this study was not sufficient to resolve dynamics related to bond dissociation. However, the transient IR experiment gave us the background and the framework for understanding the fast kinetic measurements in the visible region. Producing ultrashort UV pulses is not a standard technique but pulses as short as 20 fs at 325 nm were generated. This was the first study of transition metal carbonyl photodissociation in solution resolved with such good time resolution.

Based on transient absorption measurements and quantum chemical calculations we were able to create a possible model for the ligand exchange reaction of (*trans*-I)$Ru(dcbpy)(CO)_2I_2$ (see Fig. 5.1) Excitation with 320 nm brings the molecule in a bound dcbpy ligand centered $\pi^* \leftarrow \pi$ state. From the initially excited state internal conversion to a lower lying bound state (IC1) competes with predissociation (IC2). The observed rate constant of 1/30 fs^{-1} is then a sum of the rates of these coupled processes. In a repulsive state CO group starts to separate from the ruthenium. The reacting molecule is surrounded by the solvent molecules, that create a barrier around the solute. Only a fraction of the leaving CO groups have enough energy to overcome the barrier and escape from the solvent cage. The rest of the CO groups

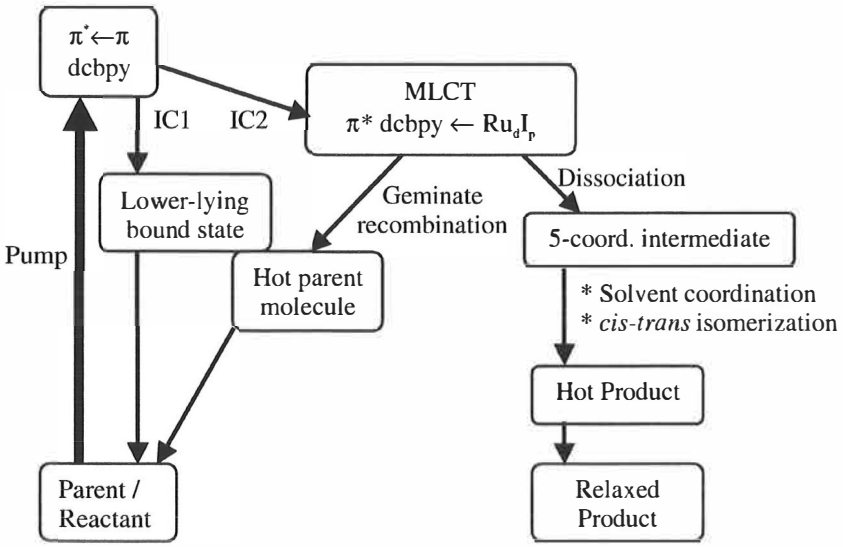

Figure 5.1: Schematic model for the reaction

bounce back and reform the parent molecules. Dissociation and recombination are also competing processes and the observed rate constant 1/62 fs^{-1} is a sum of these two processes. The reformed parent molecules are initially hot and they cool down in the picosecond timescale as their excess energy is dissipated among the several vibrational modes of the parent molecules and into the solvent. When a CO ligand has escaped outside of the solvent shell a five-coordinated intermediate complex is formed in its excited state. During the first picosecond(s) ligands of intermediate rearrange and a solvent molecule is coordinated into a vacant site of the complex. Also the newly born product (*cis*-I)Ru(dcbpy)(CO)(EtOH)I_2 is initially hot and is cooled down within few hundreds of ps.

We were able to resolve the kinetics related to dissociation but also kinetics related to conformation change and solvent attachment. We were not able to unambiguously resolve the mechanism that determines the quantum yield of the reaction. We know that the quantum yield of the reaction increases with decreasing excitation and that it is less than the maximum value of 55 % with 320 nm excitation suggested by the IR results. Most probably the non-unity quantum yield can be explained with a two step branching process: IC to dissociative state/IC to a bound state and dissociation/recombination.

Observation of the low frequency oscillations that were independent of the excitation wavelength was one of the interesting features of the reaction indicating that this component is independent of the initially excited state. The period of this oscillation is too slow to describe dissociation and it must be related to the intermediate. We assigned this component to conformational change of the five-coordinated intermediate complex. This means that the reacting system preserves its vibrational coherence during dissociation and that new vibrational modes are excited during the process.

One may conclude that combination of transient IR and transient visible spectroscopy is a suitable method to study transition metal ligand exchange reactions; the structural specificity combined with ultrafast time resolution in the visible region creates a powerful combination giving tools to understand the detailed reaction dynamics of these complexes.

It is known that in catalysis the coordinatively unsaturated transition metal carbonyls activate the bonds of the reacting species and serve as a substrate where the species may unite. Therefore, in order to understand the role and function of these complexes in catalysis it is important to understand the fundamental dynamics of the coordinatively unsaturated species. The results obtained in this work give new deep insights into the fundamental reactions of the transition metal carbonyls. Observation of (sub-)ps dynamics of five-coordinated intermediate may be generalized to reactions taking place in the catalysis. The excess energy of the complexes is rapidly dissipated into the environment (tens of ps) and this may explain the stability of the complexes. The results obtained in this thesis have been improved understanding of the basic reaction dynamics of the transition metal carbonyl complexes and I believe that the results are of help in designing new, more efficient and stable catalysts.

Bibliography

[1] T. P. Paris and W. W. Brandt. *J. Am. Chem. Soc.*, **81**, 5001, 1959.

[2] A. Juris, V. Balzani, F. Barigelletti, S. Campagna, P. Belser, and A. von Zelewsky. *Coor. Chem. Rev*, **84**, 85, 1988.

[3] D. M. Roundhill. *Photochemistry and Photophysics of Metal Complexes.* Plenum Press, New York, 1994.

[4] C. G. Garcia, J. F. de Lima, and N. Y. Murakami Iha. *Coor. Chem. Revs.*, **196**, 219, 2000.

[5] K. Kalyanasundaram. *Photochemistry of Polypyridine and Porphyrin Complexes.* Academic Press, St. Edmunsbury, 1992.

[6] M. K. Nazeeruddin, A. Kay, I. Rodicio, R. Humphry-Baker, E. Müller, P. Liska, N. Vlachopoulos, and M. Grätzel. *J. Am. Chem. Soc.*, **115**, 6328, 1993.

[7] A. Hagfeldt and M. Grätzel. *Acc. Chem. Res.*, **33**, 296, 2000.

[8] K. Kalyanasundaram and M. Grätzel, editors. *Photosensitization and Photcatalysis Using Inorganic and Organometallic compounds*, volume 14. Kluwer Academic Publishers, Dordrecht, 1993.

[9] S. A. Jackson, P. M. Hodges, M. Poliakoff, J. J. Turner, and F.-W. Grevels. *J. Am. Chem. Soc*, **112**, 1221, 1990.

[10] T. Lian, S. E. Bromberg, H. Yang, G. Proulx, R. G. Bergman, and C. B. Harris. *J. Am. Chem. Soc.*, **118**, 3769, 1996.

[11] H. Yang, K. T. Kotz, M. C. Asplund, and C. B. Harris. *J. Am. Chem. Soc.*, **119**, 9564, 1997.

[12] H. Yang, P. T. Snee, K. T. Kotz, C. K. Payne, H. Frei, and C. B. Harris. *J. Am. Chem. Soc.*, **121**, 9227, 1999.

[13] J. B. Asbury, H. N. Ghosh, J. S. Yeston, R. G. Bergman, and T. Lian. *Organometallics*, **17**, 3417, 1998.

[14] W. T. Boese and A. S. Goldman. *J. Am. Chem. Soc*, **114**, 350, 1992.

[15] S.A. Rice and M. Zhao. *Optical control of molecular dynamics.* John Wiley & Sons Inc., New York, 2000.

[16] A. Assion, T. Baumert, M. Bergt, T. Brixner, B. Kiefer, V. Seyfried, M. Strehle, and G.. Gerber. *Science*, **282**, 919, 1998.

[17] G. Rayner-Canham. *Descriptive Inorganic Chemistry.* W.H.Freeman&Co, New York, 2^{nd} edition, 2000.

[18] H. A. Nieuvenhuis, D. J. Stufkens, and A. Vlček Jr. *Inorg. Chem.*, **34**, 3879, 1995.

[19] H. Rensmo, S. Lunell, and H. Siegbahn. *J. Photochem. Photobiol. A*, **114**, 117, 1998.

[20] V Lehtovuori, P. Myllyperkiö, J. Kallioinen, M. Haukka, and J. Korppi-Tommola. *Chem. Phys.*, **295**, 81, 2003.

[21] A. Vlček Jr. *Coord. Chem. Rev.*, **177**, 219, 1998.

[22] A. Vogler and H. Kunkely. *Coord. Chem. Rev.*, **177**, 81, 1998.

[23] N. F. Scherer, J. L. Knee, D. D. Smith, and A. H. Zewail. *J. Phys. Chem.*, **89**, 5141, 1985.

[24] S. A. Trushin, W. Fuss, and W. E. Schmid. *Chem. Phys.*, **259**, 313, 2000.

[25] M. J. Paterson, P. Λ. Hunt, M. Λ. Robb, and O. Takahashi. *J. Phys. Chem. A*, **106**, 10494, 2002.

[26] S. A. Trushin, W. Fuss, K. L. Kompa, and W. E. Schmid. *J. Phys. Chem. A*, **104**, 1997, 2000.

[27] W. Fuss, W. E. Schmid, and S. A. Trushin. *J. Phys. Chem. A*, **105**, 333, 2001.

[28] L. Bañares, T. Baumert, M. Bergt, B. Kiefer, and G. Gerber. *J. Chem. Phys.*, **108**, 5799, 1998.

[29] S. K. Kim, S. Pedersen, and A. Zewail. *Chem. Phys. Lett.*, **233**, 500, 1995.

[30] M. Gutmann, M. Dickebohm, and J. M. Janello. *J. Phys. Chem. A*, **103**, 2580, 1999.

[31] M. Gutmann, J. M. Janello, M. S. Dickebohm, M. Grossekathöfer, and J. Lindener-Roenneke. *J. Phys. Chem. A*, **102**, 4138, 1998.

[32] T. P. Dougherty, T. W. Grubbs, and E. J. Heilweil. *J. Phys. Chem.*, **98**, 9396, 1994.

[33] T. Lian, S. E. Bromberg, M. C. Asplund, H. Yang, and C. B. Harris. *J. Phys. Chem.*, **100**, 11994, 1996.

[34] H. Yang, P. T. Snee, K. T. Kotz, C. K. Payne, and C. B. Harris. *J. Am. Chem. Soc.*, **123**, 4204, 2001.

[35] A. G. Joly and K. A. Nelson. *J. Phys. Chem.*, **93**, 2876, 1989.

[36] S. A. Trushin, W. Fuss, W. E. Schmid, and K. L. Kompa. *J. Phys. Chem. A*, **102**, 4129, 1998.

[37] M. Bergt, T. Brixner, C. Dietl, B. Kiefer, and G. Gerber. *J. Organomet. Chem.*, **661**, 199, 2002.

[38] Š. Vajda, P. Rosendo-Francisco, C. Kaposta, M. Krenz, C. Lupulescu, and L. Wöste. *Eur. Phys. J. D*, **16**, 161, 2001.

[39] V. Lehtovuori, P. Myllyperkiö, C. Manzoni, D. Polli, G. Cerullo, M. Haukka, J. Linnanto, and J. Korppi-Tommola. *J. Am. Chem. Soc.* submitted.

[40] A. H. Zewail. (Imperial College Press, London). chapter 1. Femtochemistry: Dynamics with Atomic Scale Resolution, pages 1–53. Nobel symposium, 1997.

[41] A. Rosa, G. Riccardi, J.E. Bearends, and D. J. Stufkens. *J. Phys. Chem. A*, **100**, 1996.

[42] T. P. M. Goumans, A. W. Ehlers, M. C. van Hemert, A. Rosa, E.-J. Baerends, and K. Lammertsma. *J. Am. Chem. Soc*, **125**, 3558, 2003.

[43] S. Záliš, I. R. Farrel, and A. Vlček. *J. Am. Chem. Soc.*, **125**, 4580, 2003.

[44] E. J. Baerends and A. Rosa. *Coord. Chem. Rev.*, **177**, 97, 1998.

[45] K. Koike, N. Okoshi, H. Hori, K. Takeuchi, O. Ishitani, H. Tsubaki, I. P. Clark, M. W. George, F. P. A. Johnson, and J. J. Turner. *J. Am. Chem. Soc.*, **124**, 11448, 2002.

[46] D. Guillamont, A. Vlček Jr., and C. Daniel. *J. Phys. Chem. A*, **105**, 1107, 2001.

[47] A. Vlček Jr, I. R. Farrel, D. J. Liard, P. Matousek, M. Towrie, A. W. Parker, D. C. Grills, and M. W. George. *J. Chem. Soc., Dalton Trans.*, page 701, 2002.

[48] S. Luukkanen, M. Haukka, E. Eskelinen, T. A. Pakkanen, V. Lehtovuori, J. Kallioinen, P. Myllyperkiö, and J. Korppi-Tommola. *Phys. Chem. Chem. Phys.*, **3**, 1992, 2001.

[49] D. F. Shriver, P. W. Atkins, and C. H. Langford. *Inorganic Chemistry*. Oxford University Press, 2 edition, 1994. 819 p.

[50] O. Rubner and V. Engel. *Chem. Phys. Lett.*, **293**, 485, 1998.

[51] R. L. Jackson. *Acc. Chem. Res.*, **25**, 581, 1992.

[52] S. Firth, W. E. Klotzbüchel, M. Poliakoff, and J. J. Turner. *Inorg. Chem.*, **26**, 3370, 1987.

[53] R. Krishnan and R. H. Schultz. *Organometallics*, **20**, 3314, 2001.

[54] S. Zhang and G. R. Dobson. *Organometallics*, **11**, 1992.

[55] E. O'Driscoll and J. D. Simon. *J. Am. Chem. Soc.*, **112**, 6580, 1990.

[56] K. T. Kotz, H. Yang, P. T. Snee, and C. B. Harris. *J. Organomet. Chem.*, **596**, 183, 2000.

[57] P. A. Anfinrud, C.-H. H Han, T. Lian, and R. M. Hochstrasser. *J. Phys. Chem.*, **95**, 574, 1991.

[58] J. D. Simon and X. Xie. *J. Phys. Chem*, **90**, 6751, 1986.

[59] T. P. Dougherty and E. J. Heilweil. *Chem. Phys. Lett.*, **227**, 19, 1994.

[60] J. C. Owrutsky and A. P. Baronavski. *J. Chem. Phys.*, **105**, 9864, 1996.

[61] M. Rini, A.-K. Holm, E. T. J. Nibbering, and H. Fidder. *J. Am. Chem. Soc.*, **125**, 3028, 2002.

[62] S. E. Bromberg, T. Lian, R. G. Bergman, and C. B. Harris. *J. Am. Chem. Soc.*, **118**, 2069, 1996.

[63] V. Lehtovuori, J. Aumanen, P. Myllyperkiö, M. Rini, E. T. J. Nibbering, and J. Korppi-Tommola. *J. Phys. Chem. A*, **108**, 1644, 2004.

[64] J. J. Turner, J. K. Burdett, R. N. Perutz, and M. Poliakoff. *Pure Appl. Chem.*, **49**, 271, 1977.

[65] T. Bultmann and N. P. Ernsting. *J. Phys. Chem*, **100**, 19417, 1996.

[66] W. T. Grubbs and E. J. Heilweil. *J. Chem. Phys.*, **100**, 4006, 1994.

[67] D. A. Steinhurst, A. P. Baronavski, and J. C. Owrutsky. *Chem. Phys. Lett.*, **361**, 513, 2002.

[68] M. W. George and J. J. Turner. *Coord. Chem. Rev.*, **177**, 201, 1998.

[69] M. Rini, J. Kummrow, J. Dreyer, E. T. J. Nibbering, and T. Elsaesser. *Faraday Discuss.*, **122**, 27, 2002.

[70] J. K. Burdett, J. M. Grzybowski, R. N. Perutz, M. Poliakoff, J. J. Turner, and R. F. Turner. *Inorg. Chem.*, **17**, 147, 1978.

[71] C. Rullière, editor. *Femtosecond Laser Pulses.* Springer, Heidelberg, 1998.

[72] J. Amesz and A. J. Hoff, editors. *Biopysical Techniques in Photosynthesis*, volume 3 of *Advances in photosynthesis.* Kluwer Academic Publishers, Dordrecht, 1996.

[73] J.-C. Diels and W. Rudolph. *Ultrashort Laser Pulse Phenomena.* Academic Press, London, 1996.

[74] E. Eskelinen, M. Haukka, T. Venäläinen, T. A. Pakkanen, M. Wasberg, S. Chardon-Noblat, and A. Deronzier. *Organometallics*, **19**, 163, 2000.

[75] M. J. Frisch, G. W. Trucks, H. B. Schlegel, G. E. Scuseria, M. A. Robb, J. R. Cheeseman, V. G. Zakrzewski, J. A. Jr. Montgomery, R. E. Stratmann, J. C. Burant, S. Dapprich, J. M. Millam, A. D. Daniels, K. N. Kudin, M. C. Strain, O. Farkas, J. Tomasi, V. Barone, M. Cossi, R. Cammi, B. Mennucci, C. Pomelli, C. Adamo, S. Clifford, J. Ochterski, G. A. Petersson, P. Y. Ayala, Q. Cui, K. Morokuma, D.K. Malick, A. D. Rabuck, K. Raghavachari, J. B. Foresman, J. Cioslowski, J. V. Ortiz, A. G. Baboul, B. B. Stefanov, G. Liu, A. Liashenko, P. Piskorz,

I. Komaromi, R. Gomperts, R. L. Martin, D. J. Fox, T. Keith, M. A. Al-Laham, C. Y. Peng, A. Nanayakkara, C. Gonzalez, M. Challacombe, P. M. W. Gill, B. G. Johnson, W. Chen, M. W. Wong, J. L. Andres, M. Head-Gordon, E. S. Replogle, and J. A. Pople. Gaussian 98 (revision a.6), 1998.

[76] S. Huzinaga, J. Andzelm, M. Klobukowsi, E. Radzio-Andzelm, Y. Sakai, and H. Tatewaki, editors. *Gaussian basis sets for molecular calculations.* Elsevier, Amsterdam, 1984.

[77] M. C. Zerner, G. H. Loew, R. F. Kirchner, and U. T. Mueller-Westerhoff. *J. Am. Chem. Soc.*, **102**, 589, 1980.

[78] J. Riedley and M. C. Zerner. *Theor. Chim. Acta*, **32**, 111, 1973.

[79] M. C. Zerner. *Reviews in Computational Chemistry*, volume 2. VCH, 1991.

[80] P.W. Atkins and J. de Paula. *Physical Chemistry.* Oxford University Press, Oxford, 7^{th} edition, 2002.

[81] R. Schinke. *Photodiccociation Dynamics.* Cambridge Monographs on Atomic, Molecular and Chemical Physics 1. Cambridge University Press, Cambridge, 1993.

[82] A.H. Zewail. *J. Phys. Chem. A*, **104**, 5660, 2000.

[83] G. Cerullo, M. Nisoli, and S. De Silvestri. *Appl. Phys. Lett.*, **71**, 3616, 1997.

[84] G. Cerullo, M. Nisoli, S. Stagira, and S. De Silvestri. *Opt. Lett.*, **23**, 1283, 1998.

[85] T. Wilhelm and E. Riedle. *Opt. Lett.*, **22**, 1494, 1997.

[86] G.M. Gale, M. Cavallari, T.J. Driscoll, and F. Hache. *Opt. Lett.*, **20**, 1562, 1995.

[87] A. Kummrow, M. Wittmann, F. Tschirschwitz, G. Korn, and E. T. J. Nibbering. *Appl. Phys. B*, **71**, 885, 2000.

[88] P. Hamm, M. Lim, and R.M. Hochstrasser. *J. Chem. Phys.*, **197**, 10523, 1997.

[89] P. Hamm, R. A. Kaindl, and J. Stenger. *Opt. Lett.*, **25**, 1798, 2000.

[90] J. Kallioinen, G. Benkö, A. P. Yartsev, J. E. I Korppi-Tommola, and V. Sundström. *J. Phys. Chem. B*, **106**, 4396, 2002.

[91] G. Benkö, J. Kallioinen, J. E. I. Korppi-Tommola, A. Yartsev, and V. Sundström. *J. Am. Chem. Soc.*, **124**, 489, 2002.

[92] N. H. Damrauer, G. Cerullo, A. Yeh, T. R. Boussie, C. H. Shank, and J. K. McCusker. *Science*, **275**, 1997.

[93] A. Vlček Jr. *Coord. Chem. Revs.*, **230**, 225, 2002.

[94] I.-R. Lee, W.-K. Chen, Y.-C. Chung, and P.-Y. Cheng. *J. Phys. Chem. A*, **104**, 10595, 2000.

[95] E. W.-G. Diau, J. L. Herek, Z. H. Kim, and A. H. Zewail. *Science*, **279**, 847, 1998.

[96] R. M. Bowman, M. Dantus, and A. H. Zewail. *Chem. Phys. Lett.*, **161**, 297, 1989.

[97] T. Baumert, M. Grosser, R. Thalweiser, and G. Gerber. *Phys. Rev. Lett.*, **67**, 3753, 1991.

[98] C.J. Bardeen, Q. Wang, and C.V. Shank. *J. Phys. Chem. A*, **102**, 2759, 1998.

[99] A. J. Wurzer, S. Lochbrunner, and E. Riedle. *Appl. Phys. B*, **71**, 405, 2000.

[100] J. Jethwa, D. Ouw, K. Winkler, N. Hartmamm, and P. Vöhringer. *Z. Phys. Chem.*, **214**(10), 1367, 2000.

[101] M. Seel, S. Engleitner, and W. Zinth. *Chem. Phys. Lett.*, **275**, 363, 1997.

[102] P. Kambhampati, D. H. Son, T. W. Kee, and P. F. Barbara. *J. Phys. Chem. A*, **104**, 10637, 2000.

Paper I

Reproduced by permission of
"Photochemical reactivity of halogen-containing ruthenium-dcbpy (dcbpy=4,4'-dicarboxylic acid-2,2'-bipyridine) compounds, *trans*(Br)-[Ru(dcbpy)$(CO)_2Br_2$] and *trans*(I)-[Ru(dcbpy)$(CO)_2I_2$] "
Luukkanen, S.; Haukka, M.; Eskelinen, E.; Pakkanen, T.A.; Lehtovuori, V.; Kallioinen, J.; Myllyperkiö, P.; Korppi-Tommola, J., *Physical Chemistry Chemical Physics*, **2001**, 3, 1992-1998.

https://doi.org/10.1039/B100659M

Paper II

https://doi.org/10.1016/j.chemphys.2003.08.008

Paper III

https://doi.org/10.1021/jp036492u

Paper IV

https://doi.org/10.1021/jp044735s